BIOLOGICAL EFFECTS OF ELECTROMAGNETIC FIELDS AT MOBILE TELECOMMUNICATION FREQUENCIES

by

ALİ İHSAN YÜREKLİ

B.S. in Physics, Boğaziçi University, 1994
M.S. in Biomedical Science, Boğaziçi University, 1997

Submitted to
the Institute of Biomedical Engineering
in partial fulfillment of the requirements for
the degree of Doctor of Philosophy
in
Biomedical Science

Boğaziçi University

İstanbul

December 2006

ACKNOWLEDGEMENTS

The work presented here was performed under Boğaziçi University Biomedical Engineering Institute supervised by Professor Mehmed Özkan. Electromagnetic exposure experiments were conducted at EMC TEMPEST Test Center of TÜBİTAK UEKAE (National Research Institute of Electronics and Cryptology). Biological parameters were analyzed at İstanbul University Cerrahpaşa Medical School laboratories. The research performed in the scope this thesis study was sponsored by Boğaziçi University Research Fund, project number: 01HX102D.

There are so many people whom I owe gratefulness.

First, I would like to express my gratitude to my thesis advisor Professor Mehmed Özkan for his judicious supervision and for never losing his hope on the accomplishment of this study. Then I would like to thank my managers at TÜBİTAK UEKAE for supporting me in academic affairs. I would also like to thank to Professor Tunaya Kalkan who guided me on biological aspects and worked with me beneficently throughout this thesis study.

My dear friend, Associate Professor Handan Tuncel, from Cerrahpaşa Medical School was helpful in many aspects until the last minute. Professor Selim Şeker, in addition to his useful comments, cordially opened his office at one phase of the study and allowed me to work there even at overtime periods. Associate Professor Hale Saybaşılı gave precious advice during progress report presentations and in journal article preparation process. Professor Koray Gümüştaş and Dr. Pınar Atukeren, from Cerrahpaşa Medical School, were very cooperative in the analysis of biochemical end-points. Dr. Haydar Durak helped on the leukocyte counts and colleagues from Cerrahpaşa Medical School Central Laboratory on urine analysis. My ex-colleague but a friend for a life-time, Mr. Mehmet Yazıcı, was a valuable partner in calculating the dosimetry of the experiment setup using numerical methods. Another contribution worth to address was from my old friend, Cardiologist Dr. Hüseyin Aksu, in performing statistical analysis.

I thank them all.

Finally, I want to thank to my family, now enlarged so as to include a dignified wife and two lovely kids. Their existence brings me the joy of life and gives me the strength to stand against difficulties.

ABSTRACT

BIOLOGICAL EFFECTS OF ELECTROMAGNETIC FIELDS AT MOBILE TELECOMMUNICATION FREQUENCIES

The ever increasing use of cellular phones and increasing number of associated base stations are becoming a widespread source of non ionizing electromagnetic radiation. The immediate biological effect of electromagnetic (EM) radiation is the generation of heat in the body and it is generally evident under high levels of electromagnetic energy. However, some biological effects are likely to occur even at low-level EM fields. In this study, a Gigahertz Transverse Electromagnetic (GTEM) test chamber was used as an exposure environment for plane wave conditions of far-field free space EM field propagation at the GSM Base Transceiver Station (BTS) frequency of 945 MHz and effects on oxidative stress in rats were investigated. Groups of young adult male Wistar albino rats were kept inside the test chamber for 7 hours/day for a period of 8 days. When EM fields at a power density of 3.67 W/m^2 (Specific Absorption Rate = 11.3 mW/kg), which is well below current exposure limits, were applied, MDA (malondialdehyde) level was found to increase and reduced glutathione (GSH) concentration was found to decrease significantly ($p<0.0001$). Additionally, there was a less significant ($p=0.0190$) increase in SOD (superoxide dismutase) activity under EM exposure, when compared to the sham exposed group. Leukocyte counts before and after the experiment and vanil mandelic acid (VMA) levels during the experiment were also assessed. We conclude that free radical mechanisms may have a probable role on the adverse effects of EM fields at mobile telecommunication frequencies.

Keywords: GSM, base station, oxidative stress, antioxidant, MDA, GSH, SOD, GTEM.

ÖZET

MOBİL HABERLEŞME FREKANSLARINDAKİ ELEKTROMANYETİK ALANLARIN BİYOLOJİK ETKİLERİ

Günümüzde kullanımları giderek yaygınlaşan cep telefonları ve sayıları gün geçtikçe artan baz istasyonları, çok yaygın elektromanyetik ışıma kaynaklarıdır. Elektromanyetik alanların birincil etkisi, biyolojik dokularda ısı oluşumudur. Bu etkinin oluşması için yüksek seviyeli elektromanyetik alanların uygulanması gerekir. Ancak, düşük seviyeli elektromanyetik alanların da, ısıl etkiler dışında bazı biyolojik etkileri oluşturması söz konusudur. Bu çalışmada, GTEM (Gigahertz Transverse Electromagnetic) test odası, 945 MHz'deki baz istasyonu ışımasının serbest uzay şartlarına uygun şekilde üretilmesi için deney ortamı olarak kullanılmış ve elektromanyetik alanların genç erişkin erkek Wistar albino sıçanlardaki oksidatif strese etkileri araştırılmıştır. Maruziyet sınırlarının oldukça altında bir seviyede, 3.67 W/m^2 güç yoğunluğunda (özgül soğurma oranı = 11.3 mW/kg) bir elektromanyetik alan uygulandığında, malon dialdehit (MDA) seviyesinin anlamlı şekilde arttığı ($p<0.0001$) ve indirgenmiş glutatyon (GSH) yoğunluğunun anlamlı şekilde azaldığı ($p<0.0001$) gözlenmiştir. Ayrıca, süperoksit dismutaz (SOD) seviyesinde de anlamlı bir artış görülmüştür ($p=0.0190$). Deney öncesi ve sonrası lökosit sayıları ile deney sırasındaki vanil mandelik asit (VMA) seviyeleri de ölçülen parametreler arasındadır. Yapılan bu çalışma, mobil haberleşme frekanslarındaki elektromanyetik alanların zararlı etkilerinde, serbest radikal mekanizmalarının muhtemel bir rolü olduğu sonucuna götürmektedir.

Anahtar Sözcükler: GSM, baz istasyonu, oksidatif stres, antioksidan, MDA, GSH, SOD, GTEM.

TABLE OF CONTENTS

Page

Page

Page

LIST OF FIGURES

Page

Page

LIST OF TABLES

Page

LIST OF ABBREVIATIONS

BSC	Base Station Controller
BTS	Base Transceiver Station
CAT	Catalase
CW	Continuous Wave
dB	Decibell
EIRP	Equivalent Isotropically Radiated Power
ELF	Extremely Low Frequency
EM	Electromagnetic
EMC	Electromagnetic Compatibility
EMF	Electromagnetic Field
FDMA	Frequency Division Multiple Access
FDTD	Finite Difference Time Domain
FEM	Finite Element Method
GSH	Reduced Glutathione
GSH-Px	Glutathione Peroxidase
GSM	Global System for Mobile communication
GSSG	Oxidized Glutathione
GTEM	Gigahertz Transverse Electromagnetic
MDA	Malondialdehyde
PNL	Polymorphonuclear Leukocyte
PUFA	Poly-Unsaturated Fatty Acid
RF	Radio Frequency
ROS	Reactive Oxygen Species
SAR	Specific Absorption Rate
SOD	Superoxide Dismutase
TDMA	Time Division Multiple Access
TÜBİTAK	Türkiye Bilimsel ve Teknolojik Araştırma Kurumu
UEKAE	Ulusal Elektronik ve Kriptoloji Araştırma Enstitüsü
VMA	Vanil (or Vanilyl) Mandelic Acid

1. INTRODUCTION

The fast growing second generation mobile phone system, Global System for Mobile Communications (GSM), has become the world's largest mobile telecommunications system, with its nearly two billion subscribers in over 200 countries. Since handheld mobile sets used for communication purposes, i.e. mobile phones, and main elements of the communication network, i.e. base stations, are transmitters of electromagnetic energy, health concerns are raised in the public.

Electromagnetic (EM) radiation produced by mobile phone and their base station antennas are in the 890 – 960 MHz frequency range for the GSM900 system. While mobile phones emit low power (2 Watts or less) EM fields in the 890 – 915 MHz range, the base station emissions are much higher in power and in the 935 – 960 MHz range. Since mobile phones are kept and used near the body, in particular near the head, emissions should be analyzed in the near field. On the other hand, base station radiation must be modeled with far field considerations. Another concern on base stations is the continuous emission of EM radiation. Therefore, residents who live close to base stations may have a bigger health concern than the casual users of the mobile phones.

There are a number of governmental and independent organizations working on the regulation of the EM radiation from mobile phones and their base stations. As a result useful guidelines and directives have been placed in act [1, 2, 3]. These guidelines, however, focus on the specific absorption rate (SAR) values, which addresses the energy deposition in the body in terms of heat. A SAR level of 4 W/kg is accepted as harmful to health. With a safety margin of 1/10, occupational exposure limit is set to 0.4 W/kg. Another asfety margin of 1/5 is applied for the general public and exposure limit is set to 008 W/kg. In May 2000, in IEGMP Mobile Phones and Health report [4], concerns were reaffirmed in the following statement, as: "…There is now scientific evidence, however, which suggests that there may be biological effects occurring at exposures below these guidelines.".

A relatively recent comprehensive survey on mobile phone health effects, published by National Radiological Protection Board (NRPB, UK) [5], summarizes 26 reports from several countries. The survey concludes that although the possibility of low level EM field exposure causing adverse health effects remain "unproven", additional well targeted, high quality research will be valuable to explore the remaining uncertainties further.

One of the areas of interest by scientists in recent years is the EM radiation induced oxidative stress in biological systems. Oxidative stress is a function of free radical acitivity in the biological system. The issue was first studied for the extremely low frequency (ELF) range, particularly for the power-line frequency magnetic fields [6, 7]. Some recent studies also address effects in radio frequency (RF) range, especially for the mobile telecommunications emissions [8, 9, 10, 11].

Free radical is a molecule or ion that has an unpaired electron in its outer orbit. Radical particles are unstable and are very reactive. Most common free radicals are produced from oxygen metabolism and are, thus, called as reactive oxygen species (ROS). Free radicals start chain reactions as the unpaired electron is transferred from one molecule to another. One known consequence of this kind of a chain reaction is the lipid peroxidation, where reactive radicals, such as NO_2^-, OH^- or $CCl_3O_2^-$, abstract an atom of hydrogen from poly-unsaturated fatty acid (PUFA) side chains in membranes or lipoproteins. This leaves an unpaired electron on carbon. The carbon radical reacts with oxygen and the resulting peroxyl radical attacks adjacent fatty acid side chains to generate new carbon radicals and so the chain reaction continues. The attack of one reactive free radical can oxidize multiple fatty acid side chains to lipid peroxides, damaging membrane proteins. This makes the membrane leaky and eventually causes complete membrane breakdown [12]. Malondialdehyde (MDA) is one of the end products of lipid peroxidation which is mostly used as an oxidative stress marker.

There are experimental evidences that oxidative stress and consequent free radical production are important causative factors in the pathology of several degenerative disorders; such as neurodegenerative diseases, carcinogenesis, atherosclerosis, hypertension and diabetic mellitus [13, 14, 15, 16]. Oxidative stress refers to the cytotoxic consequences of oxygen radicals, such as superoxide anion ($O_2\cdot^-$), hydroxyl radical ($OH\cdot$) and hydrogen peroxide (H_2O_2), which are generated as byproducts of cellular aerobic

metabolism. Oxygen radicals can attack DNA, proteins and lipid membranes, thus disturbing their physical function.

Fortunately, there are enzymatic systems to counterbalance the production of ROS. Superoxide dismutase (SOD), catalase (CAT) and glutathione peroxidase (GSH-Px) are enzymes responsible for degradation of $O_2^{\cdot -}$. While SOD converts $O_2^{\cdot -}$ to H_2O_2, GSH-Px converts H_2O_2 to water and oxygen. GSH-Px uses H_2O_2 to oxidize reduced glutathione (GSH). Decreased activity of GSH-Px leads to accumulation of H_2O_2, which in the presence of iron and copper promotes the Fenton reaction to yield $OH^{\cdot}$. Hydroxyl radical is the most reactive form of oxygen radicals that can initiate a chain reaction to generate numerous toxic reactants. GSH-Px also participates in detoxification of lipid peroxyl radicals [17, 18].

In this thesis, I submit an animal study in a confined, well-controlled environment, with an intention to investigate effects of GSM Base Transceiver Station (BTS) EM radiation on oxidative stress and generation of free radical. During this study a group of young adult male Wistar albino rats was exposed to EM fields inside a test chamber, called Gigahertz Transverse Electromagnetic (GTEM) Cell, while another group was sham-exposed under the same conditions. Malondialdehyde (MDA) levels were assessed as a marker of lipid peroxidation and the activities of GSH and SOD were determined in order to evaluate antioxidant status in the blood samples of exposed rats.

In Chapter 2, basic characteristics of electromagnetic radiation from base station antennas are explained. A summary of the outcome of recent research on biological effects of electromagnetic fields at mobile telecommmunications frequencies is also given.

Chapter 3 is dedicated to free radicals. Sources of free radicals, their effect on biological systems, antioxidant defense mechanisms and type of antioxidants are explained in this chapter.

In Chapter 4, design of the experimental setup is presented in detail. Studies performed for the dosimetric evaluation of the setup are also covered here.

In Chapter 5, biochemical analysis methods, applied during the thesis study, are briefly explained.

Results of the analysis of biological parameters after the electromagnetic exposure experiments are given in Chapter 6.

Finally, Chapter 7 gives the discussion and conclusion for this thesis study.

2. GSM RADIATION CHARACTERISTICS AND BIOLOGICAL EFFECTS STUDIES

2.1 The GSM System

GSM is the abbreviation for Global System for Mobile communication. Historically, GSM referred to the original French name, Group Speciale Mobile. This was the name of the technical study group established by the European Conference of Posts and Telecommunications (CEPT) to investigate alternative proposals for a pan-European digital cellular technology. Most of the technical standards activities of CEPT (particularly for cellular and personal communication systems) have now been taken over by the European Telecommunicatons Standards Institute (ETSI).

GSM is an open, digital cellular technology used for transmitting mobile voice and data services. GSM differs from first generation wireless systems in that it uses digital technology and time division multiple access transmission methods. GSM operates in the 900 MHz and 1.8 GHz bands in Europe and in the 850 MHz and 1.9 GHz bands in the United States of America. The 850 MHz band is also used for GSM and 3rd generation GSM in Australia, Canada and many South American countries. GSM supports data transfer speeds of up to 9.6 kbit/s, allowing the transmission of basic data services such as SMS (Short Message Service). Another major benefit is its international roaming capability, allowing users to access the same services when travelling abroad as at home. This gives consumers seamless and same number connectivity in more than 210 countries. Number of users GSM system in different regions of the world and worldwide as of mid 2006 is given in Table 2.1 with reference to GSM Association website [19].

Table 2.1 Number of GSM system users.

Market	**#Users**
World	*1,886,655,673*
Africa	150,998,455
Americas	175,908,569
Asia Pacific	713,960,992
Europe: East	269,885,831
Europe: West	383,254,293
Middle East	109,255,953
USA / Canada	83,249,151

As mentioned above, GSM technology is used on several different radio frequency bands today. However, the original GSM standard, released in 1991, was designed for use on the 900 MHz radio band [20, 21]. Main features of the GSM900 system are given in Table 2.2.

Table 2.2 Basic features of GSM900 system

Type of Service	Digital public cellular mobile radio network	**Frame Duration**	4.615 ms
Existing Applications	Portable, hand-held	**Timeslot Duration**	0.577 μs
Introduction	1991	**Modulation Technique**	GMSK
Frequency Band		**Modulation Data Rate**	270.833 kbits/s
Uplink	890 – 915 MHz	**Filter**	0.3 Gaussian
Downlink	935 – 960 MHz	**Speech Coding**	RPE-LTP 13 kbits/s
RF Carrier Spacing	200 kHz	**Voice & Data**	Data: upto 9.6 kbits/s
Multiple Access	TDMA / FDMA	**Peak Output Power (mobile unit)**	Portable: 8 W Hand-held: 2W (at the antenna connector)
Duplexing Method	FDD	**Ratio Peak/Mean Power**	8 (16 for half-rate)
Unidirectional Traffic Channel per RF carrier	8 16 (half-rate)	**Reference Standard**	ETSI 300 577 (ETSI GSM 05.05)

GSM uses a combination of both TDMA (time division multiple access) and FDMA (frequency division multiple access) techniques. The FDMA element involves the division by frequency of the (maximum) 25 MHz bandwidth into 124 carrier frequencies spaced 200 kHz apart. The carriers are then divided in time, using a TDMA scheme. The fundamental unit of time is called a burst period and it lasts for approximately 0.577 ms (15/26 ms). Eight of these burst periods are grouped into what is known as a TDMA frame. This lasts for approximately 4.615 ms (i.e. 120/26 ms) and it forms the basic unit for the

definition of logical channels. One physical channel is one burst period allocated in each TDMA frame.

The mobile phone user is given one of these slices of time for a brief pre-scheduled interval. In this manner, the capacity of the network is significantly increased over standard analog cellular phone system, which requires an entire channel for transmission.

There are different types of frame that are transmitted to carry different data, and also the frames are organised into what are termed multiframes and superframes to provide overall synchronisation [22].

2.1.1 GSM Components

A GSM network is comprised of several portions: a mobile radio part, a subscriber information part, a radio network, a switching system and network intelligence (primarily databases), as given in Figure 2.1 [21].

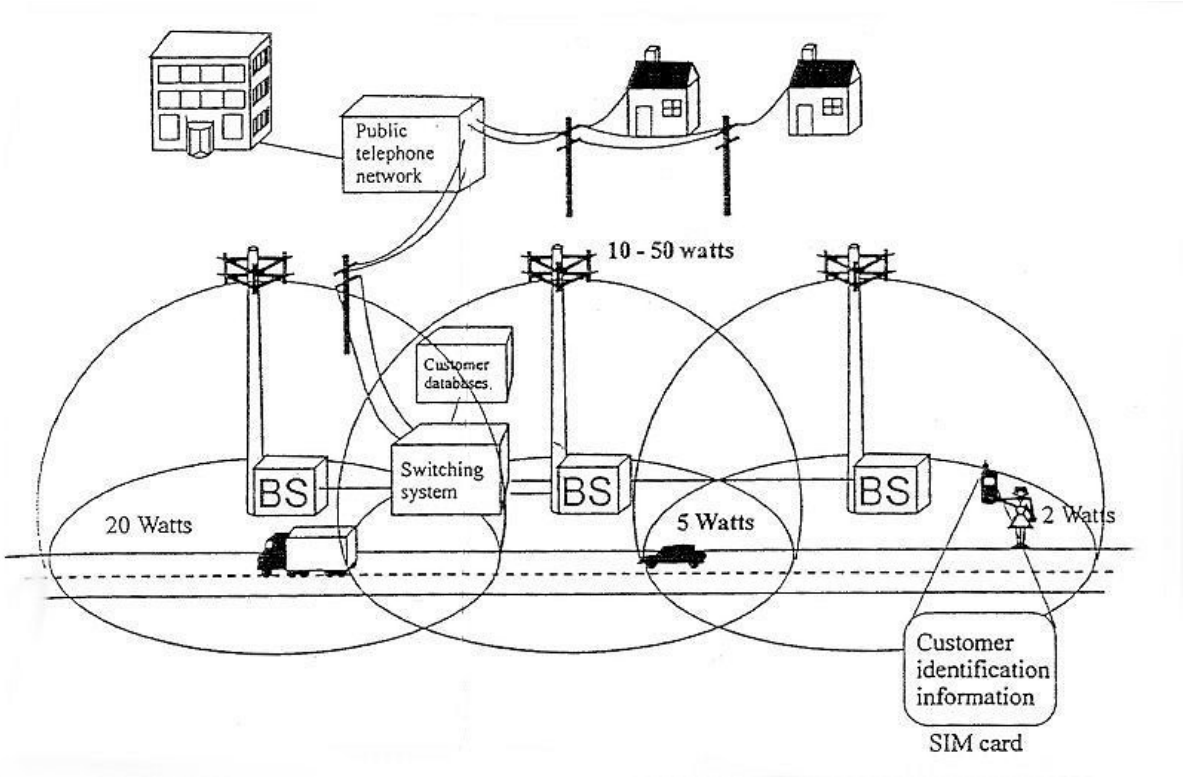

Figure 2.1 GSM components [21].

The purpose of a GSM base station is to transfer signals between mobile telephones and a network for mobile or normal telephony by means of radio frequency electromagnetic fields. Since we focus on biological effects of electromagnetic radiation from base station antennas we will provide detailed information on base stations in the following sections.

2.1.2 Base Station Subsystem

The radio parts of the GSM network equipment are contained within Base Station Subsystem (BSS). The BSS is responsible for channel allocation, link quality and power budget control, signaling and broadcast traffic control, frequency hopping, handover initiation, etc. [22]. The Base Station Subsystem is divided into two main parts: the Base Transceiver Station (BTS) and the Base Station Controller (BSC). The BTS comprises several base radio transceivers. Each transceiver consists of a transmitter and a receiver which has a duplicated “front end” to match up with the two receiving antennas used in the base antenna assembly. The BSC comprises a control computer, data communication facilities, and multiplexing and demultiplexing equipment. The BSC can control the radio power levels of the various transceivers in the BTS, and also can autonomously control the mobile stations’ radio transmitter power levels as well.

Figure 2.2 shows a basic diagram of a GSM base station subsystem. The BTS consists of transmitters, receivers, antenna assembly, power supplies and test circuits. In this diagram BSC is located at the base station. Each transmitter operates on a different radio carrier frequency [21].

Each base station is a low power radio station that serves users in a small geographic region called a cell as depicted in Figure 2.3 [23]. The location of each base station is determined by two different needs on the part of the system. One is to provide adequate coverage (i.e. provide adequate signal strength throughout the entire service area). The second is to provide adequate capacity (i.e. provide enough free channels to accommodate any user who might wish to use the system). As a system grows, base stations are installed closer together (to increase capacity) but operated at lower power levels (to prevent interference among base stations). Thus, in urban areas base stations are closer together, but operated at lower power levels, than in rural areas where the cells tend to be larger [24].

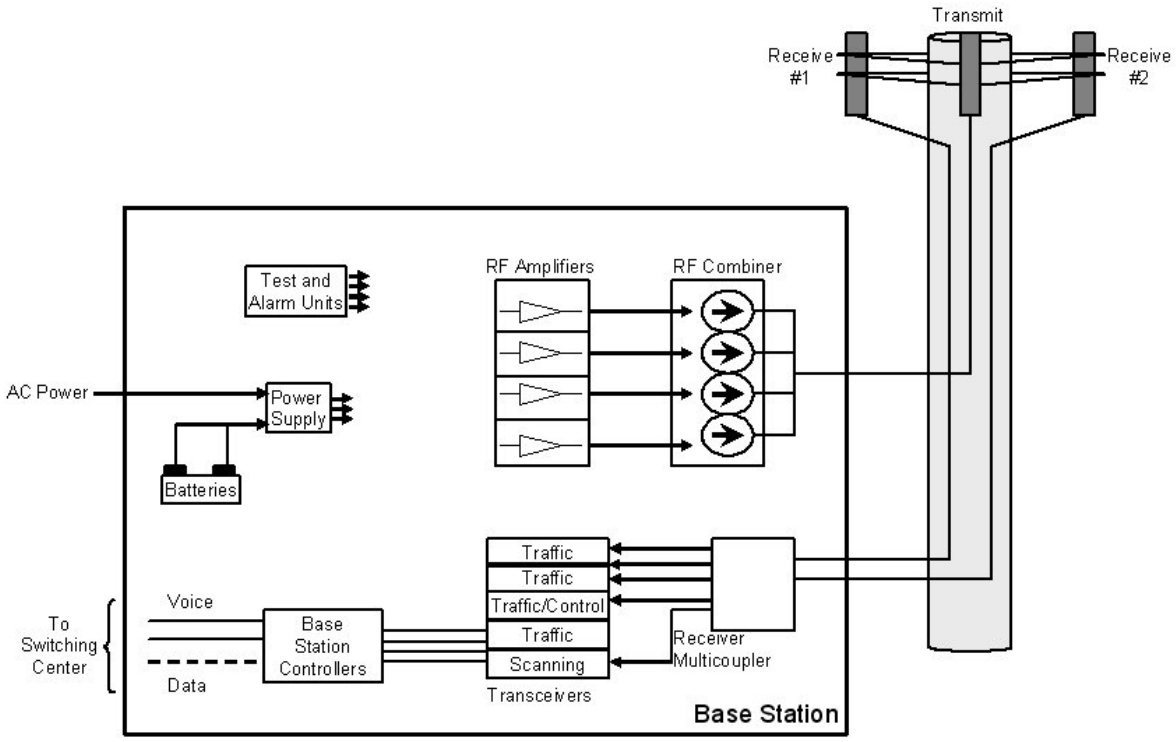

Figure 2.2 The Base Station Subsystem [21].

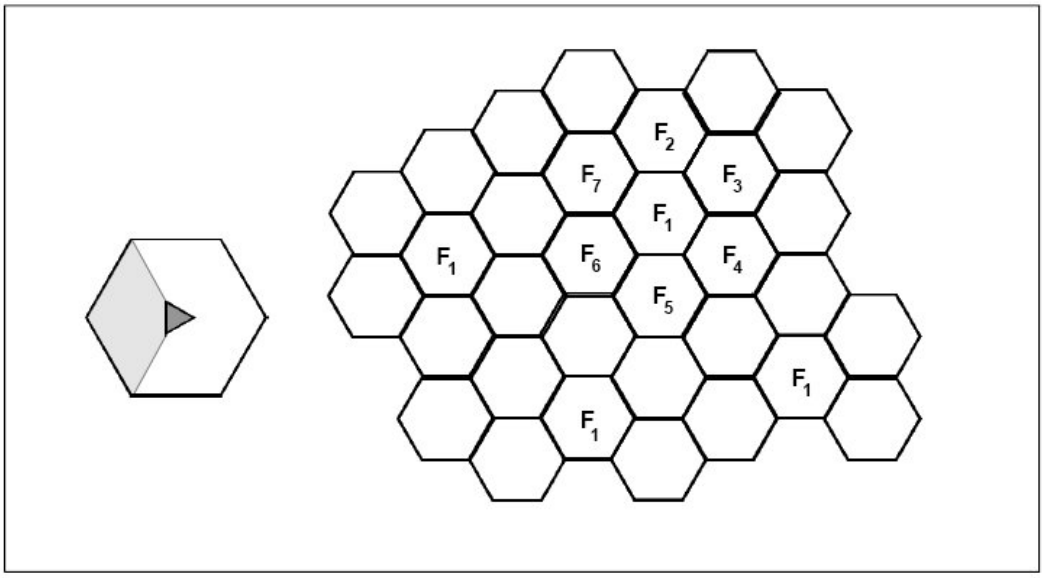

Figure 2.3 Schematic representation of a network's cellular structure. Neighbouring cells have different frequencies (F1 through F7). On the left: the position of the base station within the cell and the area covered by one antenna [23].

There are three types of cells: macrocells, microcells and picocells. A macrocell provides the main coverage in a mobile network. The antennas for macrocells are mounted on ground-based masts, rooftops and other existing structures. They must be positioned at a height that is not obstructed by surrounding buildings and terrain. Macrocell base stations have a typical power output of tens of watts.

Microcells provide infill radio coverage and additional capacity where there are high numbers of users within macrocells. The antennas for microcells are mounted at street level, typically on the external walls of existing structures, lamp posts and other street furniture. The antennas are smaller than macro cell antennas and, when mounted on existing structures, often blend in with building features to minimize visual impact. Typically, microcells provide radio coverage across smaller distances and are placed 300 m – 1000 m apart. They have lower outputs than macrocells, usually a few watts.

A picocell provides more localized coverage than a microcell. They are normally found inside buildings where coverage is poor or where there are a high number of users, such as airport terminals, train stations or shopping centers [25].

Maximum output power levels for different classes of base station antennas are given in Table 2.3 [26].

Table 2.3 Maximum output power specified for different tranceiver classes of GSM base station.

Base Station Classification	**Transceiver Power Class**	**Maximum Output Power (W)**	
		GSM900	**GSM1800**
Normal BTS	1	320 – (<640)	20 – (<40)
	2	160 – (<320)	10 – (<20)
	3	80 – (<160)	5 – (<10)
	4	40 – (<80)	2.5 – (<5)
	5	20 – (<40)	
	6	10 – (<20)	
	7	5 – (<10)	
	8	2.5 – (<5)	
Micro BTS	M1	(>0.08) – 0.25	(>0.5) – 1.6
	M2	(>0.025) – 0.08	(>0.16) – 0.5
	M3	(>0.008) – 0.025	(>0.05) – 0.16
Pico BTS	P1	(>0.02) – 0.1	(>0.04) – 0.2

Since cellular radio is a duplex system, good performance is required in both transmitting and receiving directions. Such a performance depends on many variables over

which the designer or the operator has control, such as type of antenna, gain, bandwidth, height, input impedance, mechanical rigidity, ground plane, coverage pattern, available power to drive it, application of simple of multiple antenna configuration, and polarization. Other variables where the designer has no control are topography between the BTS and the mobile station (MS) as well as the speed and direction of the MS if on vehicle [27].

2.1.2.1. Antenna System. The antenna system converts radio frequency (RF) electrical current signals to and from electromagnetic waves (radio signals). The base antennas assembly normally consists of one transmitting antenna and two receiving antennas in each sector. The use of two receiving antennas is related to a technique called receive diversity which improves the base receiver performance. Diversity reception reduces the effects of radio signal fading (called Rayleigh fading).

The shielding metal in a sectored antenna is described as a "passive" element of the antenna assembly because it is not connected electrically to the radio equipment, as the "active" antenna elements are. The shielding does its job only because of a surface interaction of reflection of the radio waves. In sectored cells, the shielding reduces the interference to and from other cells which use the same carrier frequency/frequencies as this sector, but are geometrically to the side or back, as seen by this antenna assembly.

2.1.2.2. Antenna Directivity. There are two methods for making a highly directional narrow beam angle assembly for cellular systems. One method is simple but not always practical. It involves making a very large assembly with very big shielding panels on the back and side areas. Unfortunately, size limitations make this impractical in many cases. The back and side lobes becomes narrower in angle and further separated as larger and larger shields are used, but they do not disappear completely, so there are still problem regions of undesired radio signal coverage.

A second method uses antenna assemblies with multiple active antenna elements. The radio carrier frequency signals in these various elements are controlled in their phase or relative time delay. As a result, the directional pattern is also controlled. Radio signal strength in certain directions is strong, because the waves from the various active antenna elements are in phase and reinforce each other when traveling in that direction. In contrast, radio signal strength in certain other directions is weak, because the waves from the various active antenna elements are out of phase and either fully or partially cancels each

other out when traveling in such a direction. The ratio of the desired main beam power to the undesired back or side lobe power can be controlled better than a passive antenna [21]. Typical radiation patterns of a base station antenna are given in Figure 2.4 [28].

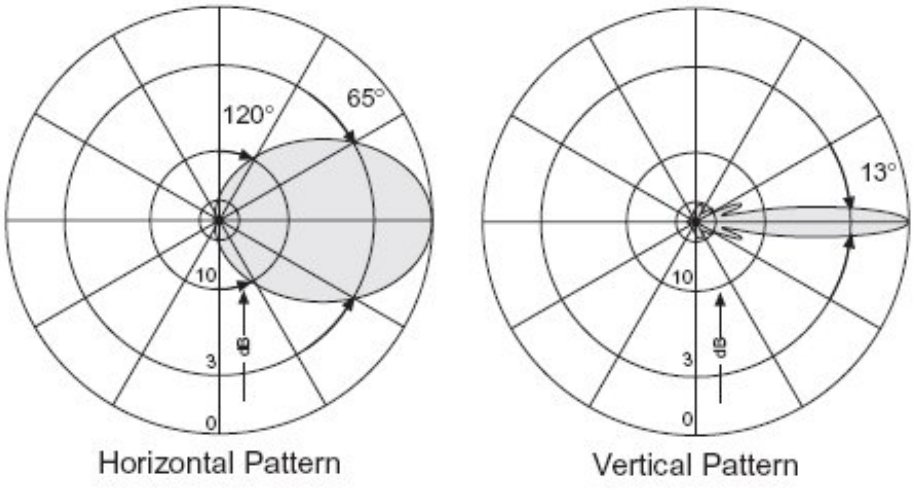

Figure 2.4 Radiation pattern of a typical base station antenna in horizontal and vertical planes [28].

2.2 Electromagnetic Radiation from Base Station Antennas

The determination of the exposure next to mobile communication base stations under real life conditions needs to consider several aspects. The RF field distribution depends on several environmental factors, field levels are varying in space and time. Multipath propagation and fading effects lead to scenarios that are often not easy to reproduce leading to large uncertainty budgets [29].

The base stations serving macrocells are either mounted on free-standing towers, typically 10-30 m high, on short towers on top of buildings, or attached to the side of the buildings.

Antennas are generally designed to serve a 120^{o} sector. A large proportion of the power is concentrated in an approximately horizontal beam typically about 6^{o} wide in the vertical direction. Rest of the radiation goes into side lobes which are weak when compared to the main beam. The main beam is tilted slightly downwards and reaches the ground at 50 – 200 m.

The RF radiation from the base station antennas is limited by defining the maximum "equivalent isotropically radiated power (EIRP)" which is the power that would have to be emitted equally in all directions to produce a particular intensity. The ratio of the EIRP to the total power output is called the gain of the antenna. For a 120^o sector antenna the gain is usually between 40 and 60.

As a result of setting the maximum EIRP at 1500 W per frequency channel, maximum radiated power from a 900 MHz base station system is less than 120 W. The total radiated power emitted from an antenna is generally limited by the characteristics of the equipment to somewhat 70 W. Total radiated power can be assumed as 60 W for general calculations.

Maximum intensity in the main beam at point on the ground 50 m from a 10 m tower carrying an antenna transmitting 60 W into a 120^o sector is about 100 mW/m^2. This corresponds to oscillating electric and magnetic fields of about 5 V/m and 0.02 μT.

The emission from a mobile phone is essentially at one frequency and that from a base station is at several specific frequencies, and in both cases, the waves have the relatively long coherence time of around 4μs. The coherence time is the average time between random phase changes, which is the result of phase modulation [4].

2.2.1 Results of Sample Measurements

Results of electromagnetic field measurements around two base stations operating in the 900 MHz band in İstanbul are given in this section. One of the measurement was performed around a rooftop antenna while the other was performed around a mast or tower type antenna.

The first group of antennas measured is built on the roof of a building (Figure 2.5). Antennas are at about 25 m above the street level. Three antennas measured are sector type antennas which are located side by side (i.e. linearly) rather than arranged around a mast. Antennas are Kathrein model 732448 which are vertically polarized, with half-power beam width of 65^o and 15 dBi gain. Since the lower edges of the antennas are 265 cm above the roof level and the length of the antennas are 130 cm, we expect maximum radiation at around 330 cm from roof level which corresponds to the middle point of the antennas. Electric field level measurements were performed using Acterna (formerly Wandel

Goltermann) EMR-300 field meter with a probe in the 100 kHz - 3 GHz frequency range. Every measurement point in Figure 2.6 represents the electric field level averaged over 6 minutes.

Figure 2.5 Three sector antennas on top of a roof.

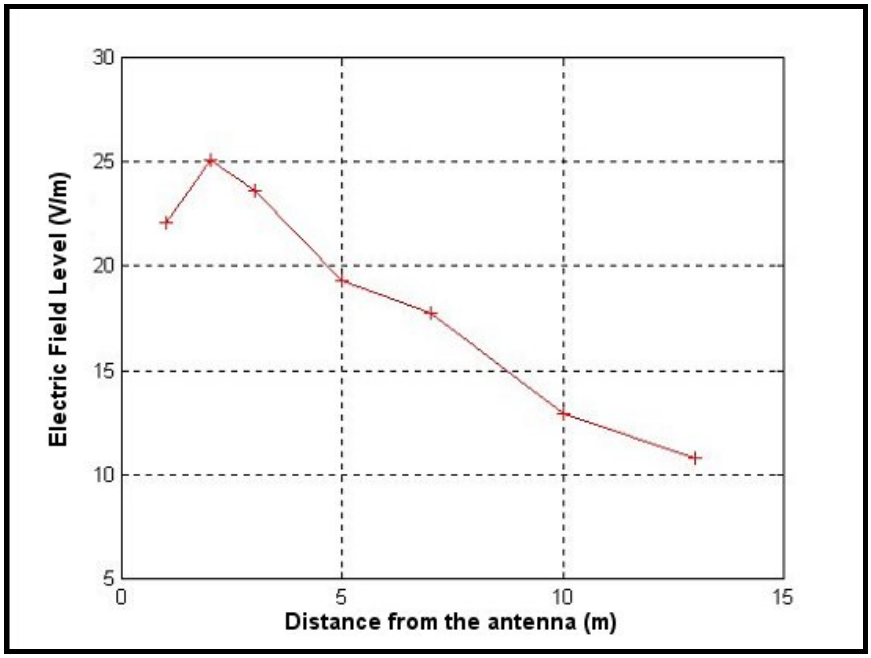

Figure 2.6 Variation of electric field with increasing distance from the rooftop antenna group.

The second measurement was performed around a mast type base station as depicted in Figure 2.7. This base station was about 20 m high from the ground level. The electric field measurements were performed using the same type of instruments but this time electric field probe was located at 160 cm above ground, with reference to regulations [3]. Variation of electric field level with increasing distance from the antennas mast is given in Figure 2.8.

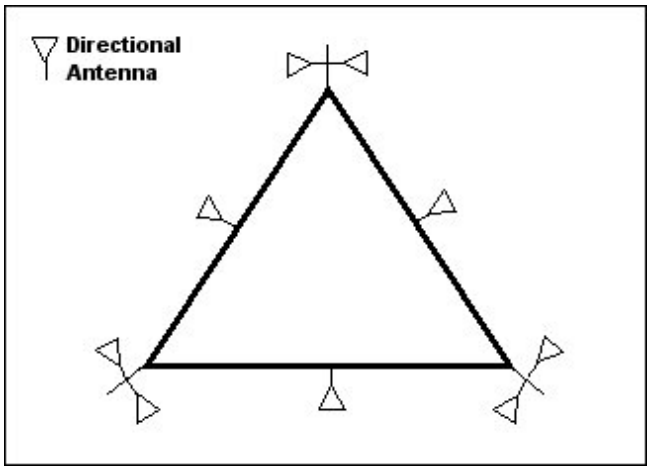

Figure 2.7 Representation of arrangement of antennas around a mast structure.

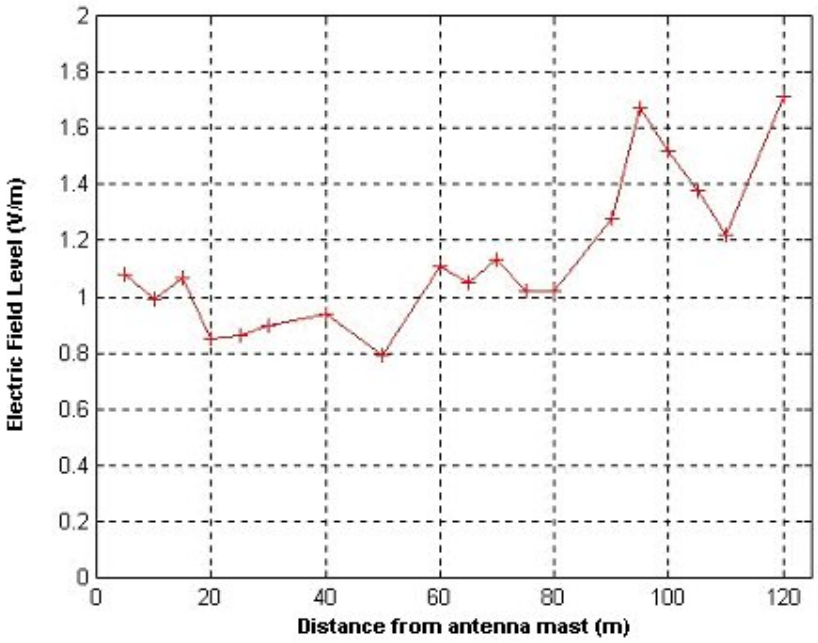

Figure 2.8 Variation of electric field level with increasing distance from the antenna mast.

Results of this two measurements show that, at the street level, electric field levels emitted from base station antennas mounted on high masts are below current public exposure limits. Public exposure limits may be exceeded on rooftop antennas when the subject is inside the main beam and at 2 - 3 meters vicinity of the antennas.

2.2.2 Results of Base Station Measurements Worldwide

Many measurement campaigns have been held in different regions of the world for the measurement of electromagnetic field levels around base station antennas. The outcome of some of these measurements are summarized in Table 2.4 below [26, 29].

Table 2.4 Results of electric field level measurements around base stations in different countries.

Country	**Organization**	**E- Field Level (V/m)**		**Scenario**
		Max	**Min**	
Germany	Regulierungsbehörde für Telekommunikation und Post (RegTP)	7.27	0.00524	No distinction between 900 and 1800 MHz
Liechtenstein	Amt für Kommunikation	6.44	0.02	No distinction between 900 and 1800 MHz
Belgium	Belgian Institute for Postal services and Telecommunications (BIPT)	19.71	0.051	Max level at 7 m, rural outdoor. Min level at rural indoor.
France (*)	National Agency of Frequecies (ANFR)	0.78	-	900MHz band, urban.
		2.52	-	1800 MHz band, urban.
Switzerland	Office of Communications (OFCOM)	3.865	0.0368	At 13 sites randomly selected.
United Kingdom	National Radiological Protection Board	2 % (**)	0.002 % (**)	At 20 microcell and picocell base stations.

(*) Mean value for a single frequency in rural areas is 0.13 V/m.
(**) Power density level given with reference to ICNIRP limit.

2.3 Basic Information Regarding Biological Effects Studies

There are many studies published in the scientific literature dealing with the biological effects of electromagnetic fields. The history of these studies goes back to 1950s where main concern was the exposure of military personnel to high-power navigation and communication transmitters, like radars and long-range radios. While the interest was focused on exremely low frequency (ELF) EM radiation from powerlines in 1980s and beginning of 1990s, research on radiofrequency electromagnetic fields has gained pace after the introduction of personal communication systems at the last years of the second millennium. Remember, we have given some information in Introduction chapter, so we will give some additional and useful information on different adpects of the subject in the following sections.

2.3.1 Types of Studies

Biological effects studies can be classified into four groups according to the characteristics of the experiment or research study performed.

Epidemiological studies provide the most direct information on long-term health effects of any potential harmful agent. To assess any damage to health generally requires long follow-up, frequently for many years. A period of ten years may be regarded a minimum period of follow-up for the identification of any long term health effects in exposed groups. In addition, epidemiological studies do not have a high sensitivity for detecting subtle effects.

Human volunteer studies are important in enabling transient physiological phenomena, such as effects on sleep patterns or on particular aspects of cognitive function, to be studied. But they are limited in the sense that they can be applicable only to healthy adults and for harmless effects.

Animal studies are frequently used to complement epidemiological studies. They are of generally shorter duration and have the advantage that they can use a homogenous population exposed under well-controlled conditions. A range of exposure conditions can be used, and exposures are well quantified, allowing studies to be replicated. The

disadvantage is that the results obtained cannot necessarily be extrapolated readily to human populations.

Cellular, or *in vitro*, studies are valuable for examining the mechanisms involved in any interactions with body tissues. They are most usefully employed to understand demonstrated effects and have been particularly valuable through modern genetic analysis in understanding factors influencing the sensitivity of tissues to chemical or biological hazards [5].

Extensive epidemiological and animal studies commonly expected to provide the answer as to whether or not electromagnetic fields (EMF) might be hazardous are in progress. However, this approach alone might not be able to provide certain evidence whether EMF can or cannot contribute to the pathogenesis of diseases such as cancer or neurodegenerative disorders. The low sensitivity of the epidemiological methodology in detecting low risk associations is probably insufficient to reliably identify any risk to health caused by EMF. Therefore, although epidemiological studies will be needed to ultimately validate the extent of any potential health hazard of EMF, such research must be supplemented and supported by data from animal and in vitro studies. Therefore, in vitro studies using the most modern molecular biological techniques such as genomics and proteomics are urgently needed in order to create at least a hypothetical basis for the understanding of disease development through EMF-exposure. If it can be determined that such a basis exists, it becomes even more important, to search for marker substances which are specific for EMF exposure. Such marker substances could considerably increase the accuracy of epidemiological studies, so that even a low health risk due to EMF exposure would not escape epidemiological detection [30].

2.3.2 Biological Effect vs. Health Effect

It is important to distinguish between biological or physiological effects and health effects. If an effect of an electromagnetic field has been demonstrated in experimental research on an isolated biological system, for instance an effect on cultured cells, this does not necessarily imply that exposure to such a field will lead to adverse effects for the health of the organism as a whole. Nor, in the absence of supporting evidence, should effects detected by sensitive measurement methods, such as subtle changes in reaction

speed or in the natural pattern of brain waves during sleep in humans, be regarded as harmful to health. The reason for this is that the human body has a great capacity for adequately processing external influences and, if necessary, effectively resisting them (with the aid of the immune system), compensating for them (homeostasis) or successfully adapting to them (specifically with the nervous and the endocrine systems) [4, 31].

The existence of an effect, whether a biological effect or an effect on health, only to be scientifically demonstrated in the event of compliance with the following objective requirements, which encompass the criteria formulated by A.B. Hill in his book "Principles of Medical Statistics" for epidemiological research:

- the research has been published in internationally refereed journals generally acknowledged in the scientific community as being of adequate quality;
- the research is of adequate quality according to prevailing standards in the scientific community;
- the results of the research have proven to be reproducible (in the case of laboratory research) or consistent (in the case of epidemiological research) on the basis of research as referred to under the first two items above conducted by other, independent researchers;
- the research result has been substantiated by quantitative analysis, leading to the conclusion that a statistically significant correlation exists between exposure and effect; in the case of epidemiologic al research, a causal link becomes more plausible as the association becomes stronger;
- the strength of the effect is related to the strength of the stimulus, i.e. there is a dose-response relationship; this need not always be the kind of relationship in which a stronger stimulus produces a stronger effect, but may also entail a resonance effect, in other words the maximum effect is produced by a specific stimulus, while stimuli that are stronger or weaker than this produce a lesser effect [31].

2.3.3 Conclusion of Recent Review Reports

There are a number of review reports published by different organizations worldwide in recent years. These reports review the scientific literature and evaluate their

findings in order to draw a conclusion and give advise to the public, government, industry, etc.

A comprehensive report was prepared by UK Independent Expert Group on Mobile Phones (IEGMP) chaired by Sir William Stewart in 2000 [4]. This group reviewed the literature and consulted related parties, like experts, members of the public, government and industry. Stewart report encouraged further well-planned research on the subject. In 2004, Sienkiewicz and Kowalczuk [5] investigated more than 20 individual reports published by national or international committes published since 2000. They brought the information from these various sources together and highligted commonality or differences in opininon. Here are verses from their summary of conclusions and recommendations:

"Overall, the reports acknowledge that exposure to low level RF fields may cause a variety of subtle biological effects on cells, animals or humans, particularly on brain activity during sleep, but the possibility of exposure causing adverse health effects remains unproven. Nevertheless, these reports suggest additional well-targeted, high quality research would be valuable to explore remaining uncertainties further. Such studies also provide reassurance to the public and help to address concerns about health. These reports stress that very low level exposures, typical of base stations, are extremely unlikely to cause any effects on biophysical grounds, whereas localized exposures, typical of those from mobile phones, may induce effects as a result of mild heating of superficial tissues close to the handset.

…

The effects of exposure to pulsed fields have received limited international attention. The main problem is the lack of an accepted biological model that shows consistent sensitivity to low level RF fields; without this model, it is not possible to examine and compare the effects of different signal modalities. Overall the evidence that modulated fields preferentially affect biological processes is fairly inconsistent and no expert groups appear to have identified any mechanism whereby modulation could cause increased effects. US National Council on Radiation Protection and Measurements (NCRP) noted that, some but not all, studies suggest modulation-specific effects may occur, with pulsed fields generally more effective than unmodulated fields, but many of these require exposures well above guideline values."

3. FREE RADICALS AND ANTIOXIDANT DEFENSE MECHANISMS

3.1 Free Radicals

3.1.1 Definition

Free radicals are atoms or molecules which have unpaired electrons on their outer orbits, thus have very reactive nature. The unpaired electrons in their outer shells do not affect the charge on the resultant molecule. Free radicals can be negatively charged, positively charged or electrically neutral. This is because charge is concerned with the number of negatively charged electrons in relation to the positively charged protons whereas free radicals are related only to the spatial arrangement of the outer electron [32].

Atomic structure consists of a nucleus and a number of electrons around it. Electrons are located according to their energy levels and move in paths called orbitals. In every orbital there can be two electrons each of which turns around itself but in the opposite direction of the other. In accordance with that rule, firstly electrons of the same turning direction, i.e. spin, fills the orbitals one by one. Then, as the atomic number increases, electrons of the opposite direction fills the orbitals in the same order.

Oxygen atom has atomic number of 8, thus, has 8 electrons. The most important orbital in oxygen molecule is the 2p which is occupied by two electrons of the same spin. When one of the electrons in these orbitals moves to the other orbital or has different spins in different orbitals, singlet oxygen is formed. When one or more orbitals are occupied by electrons of opposite spin, radicals are obtained. There are a few oxygen molecules which can be obtained from natural oxygen molecule (Figure 3.1) [33].

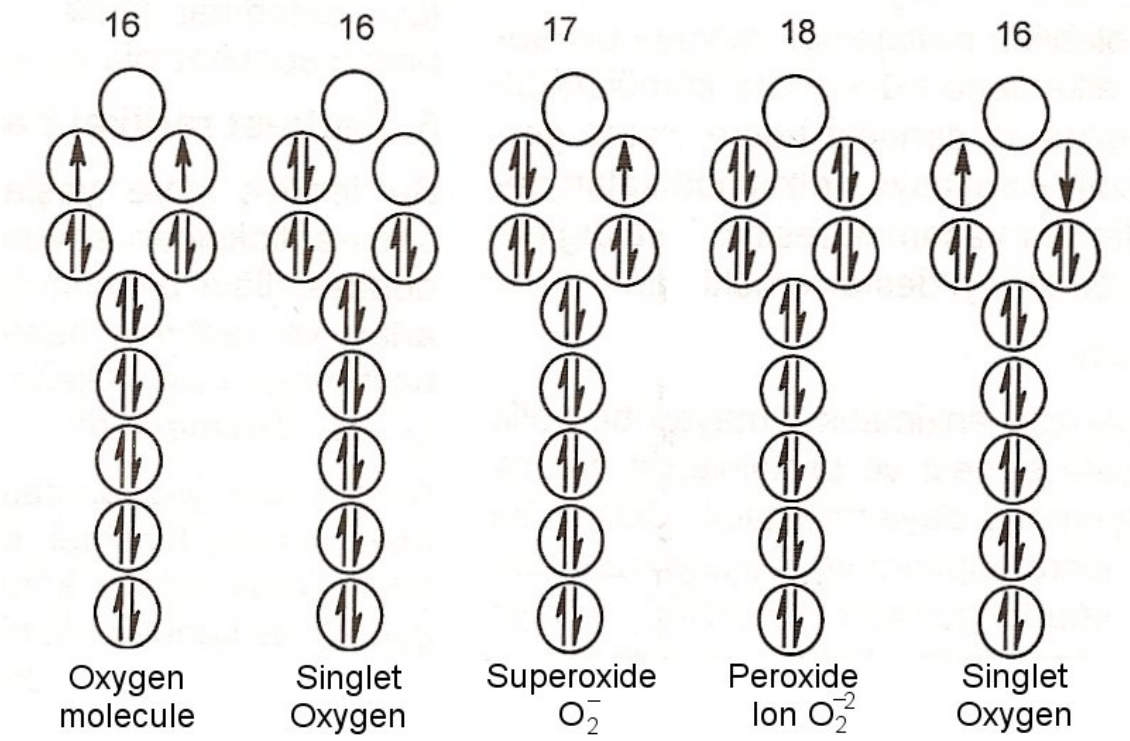

Figure 3.1 Electron distribution of oxygen molecule and oxidant molecules that are formed [33].

Free radicals can be formed in three ways:

1. Homolytic fission of covalent bonds

After the homolytic fission of a covalent bond each of the paired electrons stays in different parts.

$$X{:}Y \rightarrow X\cdot + Y\cdot$$

2. Electron loss of a molecule

When an electron is moved from one of the atoms that comprises the molecule, radicals are formed.

$$X \rightarrow X\cdot + e^-$$

3. Addition of an electron to a molecule

When an electron is added to the structure of a molecule, reactive species are formed.

$$X + e^- \rightarrow X\cdot^-$$

Since free radicals don't have a balance between the negatively charged electrons and positively charged nucleus, they are very reactive. Free radicals sometimes give their excessive electron to another molecule and sometimes take electrons from other molecules and form electron pairs. As a result, a non-radical structure turns into a radical by losing its electron.

In mammals which have aerobic metabolism, free radicals are derived from oxygen (Table 3.1). But there are also carbon and sulphur centered radicals. Oxygen as a vital element for life changes into water after a series of reactions. Cellular energy is created by these reactions. However, about 1-3% of oxygen can not be transformed into water and superoxide anion and hydoxyl radical are formed.

All aerobic cells produce radicals at certain levels. Electron transport chain reactions in the mitochondria, oxidase system in the endoplasmic reticulum, activity of enzymes like xanthine oxidase, dopamin-β-hydroxilase, D-amino acid oxidase in the cytoplasma, activity of NADPH oxidase, prostaglandin synthetase and lipoxigenase in the cell membrane and metabolic events in the liposomes are the reactions that result in the formation of free radicals [32].

Table 3.1. Oxygen-derived compounds.

Radicals		**Non-radicals**	
Hydroxyl	(HO·) or (·HO)	Hydrogen peroxide	(H_2O_2)
Alchoxyl	(RO·)	Singlet oxygen	($*O_2$)
Peroxyl	(ROO·)	Ozone	(O_3)
Superoxide	($O_2·^-$)	Hypchloric acid	(HOCl)
Nitric oxide	(NO·)	Lipid hydroperoxide	(LOOH)
Nitrogen dioxide	(NO_2·)	Peroxynitrite	($ONOO^-$)

Free radical formation reactions are given in Figure 3.2 in detail [34].

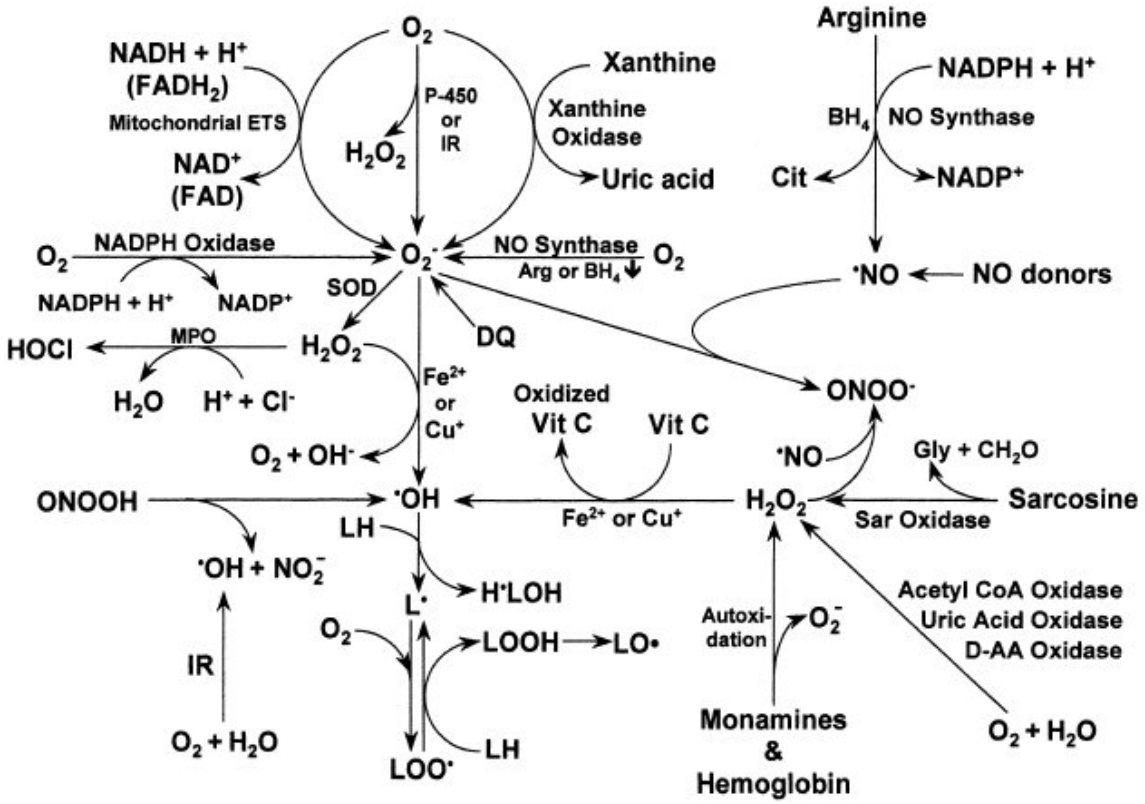

Figure 3.2 Production of oxygen and nitrogen free radicals and other reactive species in mammalian cells. AA, amino acid; Arg, L-arginine; BH_4, (6R)-5,6,7,8,-tetrahydro-L-biopterin; CH_2O, formaldehyde; Cit, L-citrulline; DQ, diquat; ETS, electron transport system; FAD, flavin adenine dinucleotide (oxidized); $FADH_2$, flavin adenine dinucleotide (reduced); Gly, glycine; H_2O_2, hydrogen peroxide; HOCl, hypochlorous acid; H•LOH, hydroxy lipid radical; IR, ionizing radiation; L•, lipid radical; LH, lipid (unsaturated fatty acid); LO•, lipid alkoxyl radical; LOO•, lipid peroxyl radical; LOOH, lipid hydroperoxide; MPO, myeloperoxidase; NAD^+, nicotinamide adenine dinucleotide (oxidized); NADH, nicotinamide adenine dinucleotide (reduced); $NADP^+$, nicotinamide adenine dinucleotide phosphate (oxidized); NADPH, nicotinamide adenine dinucleotide phosphate (reduced); •NO, nitric oxide; O_2^-, superoxide anion radical; •OH, hydroxyl radical; $ONOO^-$, peroxynitrite; P-450, cytochrome P-450; PDG, phosphate-dependent glutaminase; Sar, Sarcosine; SOD, superoxide dismutase; Vit C, vitamin C; Vit E, vitamin E (α-tocopherol) [34].

3.1.2 Sources of Free Radicals

Free radicals may result from a number of endogenous and exogenous sources.

Endogenous Sources

Autoxidation of some molecules, like haemoglobin, myglobin and thiol, in a rection reaction results in the reduction of the oxygen diradical and the formation of reactive oxygen species [35].

A variety of enzyme systems is capable of generating significant amounts of free radicals, including xanthine oxidase (activated in ischemia-reperfusion), prostaglandin synthase, lipoxygenase, aldehyde oxidase, and amino acid oxidase.

Respiratory burst is a term used to describe the process by which phagocytic cells consume large amounts of oxygen during phagocytosis. Between 70 and 90% of this oxygen consumption can be accounted for in terms of superoxide production [36].

Subcellular organelles such as mitochondria, chloroplasts, microsomes, peroxisomes and nuclei have been shown to generate $O_2\cdot^-$ and this is easily demonstrated after the endogenous superoxide dismutase has been washed away [37].

Ischemia confers a number of effects all contributing to the production of free radicals. Normally xanthine oxidase is known to catalyze the reaction of hypoxanthine to xanthine and subsequently xanthine to uric acid. This reaction requires an electron acceptor as a cofactor. During ischemia two factors occur, first the production of xanthine and xanthine oxidase are greatly enhanced. Second, there is a loss of both antioxidants superoxide dismutase and glutathione peroxidase. The molecular oxygen supplied on reperfusion serves as an electron acceptor and cofactor for xanthine oxidase causing the generation of the $O_2\cdot^-$ and H_2O_2. Strenuous exercise has been proposed to activate xanthine oxidase-catalyzed reactions and generate free radicals in skeletal muscle and myocardium.

Finally, transition metals ions such as iron and copper play a major role in the generation of free radicals and the facilitation of lipid peroxidation. Transition metal ions participate in the Haber-Weiss reaction that generates $OH\cdot$ from $O_2\cdot^-$ and H_2O_2.

$$O_2^- \cdot + H_2O_2 \xrightarrow{Fe^*} OH\cdot + OH^- + O_2$$

The Haber-Weiss reaction accelerates the nonenzymatic oxidation of molecules such as epinephrine and glutathione.

Exogenous Sources

A number of drugs can increase the production of free radicals in the presence of increased oxygen tensions.

Radiotherapy may cause tissue injury that is caused by free radicals. Electromagnetic radiation (X rays, gamma rays) and particulate radiation (electrons, photons, neutrons, alpha and beta particles) generate primary radicals by transferring their energy to cellular components such as water.

Tobacco smoke oxidants severely deplete intracellular antioxidants in the lung cells in vivo by a mechanism that is related to oxidant stress. It has been estimated that each puff of smoke has an enormous amount of oxidant materials.

Inhalation of inorganic particles also known as mineral dust (e.g. asbestos, quartz, silica) can lead to lung injury that seems at least in part to be mediated by free radical production.

Ozone is not a free radical but a very powerful oxidizing agent. Ozone (O_3) contains two unpaired electrons and degrades under physiological conditions to ·OH, suggesting that free radicals are formed when ozone reacts with biological substrates.

In addition, a wide variety of environmental agents including photochemical air pollutants as pesticides, solvents, anesthetics, exhaust fumes and the general class of aromatic hydrocarbons, also cause free radical damage to cells.

3.1.3 Biological Effects of Reactive Oxygen Metabolites and Cellular Damage

Free radicals cause cellular damage by affecting cellular structures (Figure 3.3) [33]. Free radicals have very short lifetimes but can react with almost any molecule, like proteins, lipids, carbohydrates and DNA, in their vicinity,.

Aminoacids like prolin, histidin, arginin, cystein and methionine are prone to radical damage. Oxidation of these aminoacids cause the disintegration of proteins, formation of cross bonds, and aggregation.

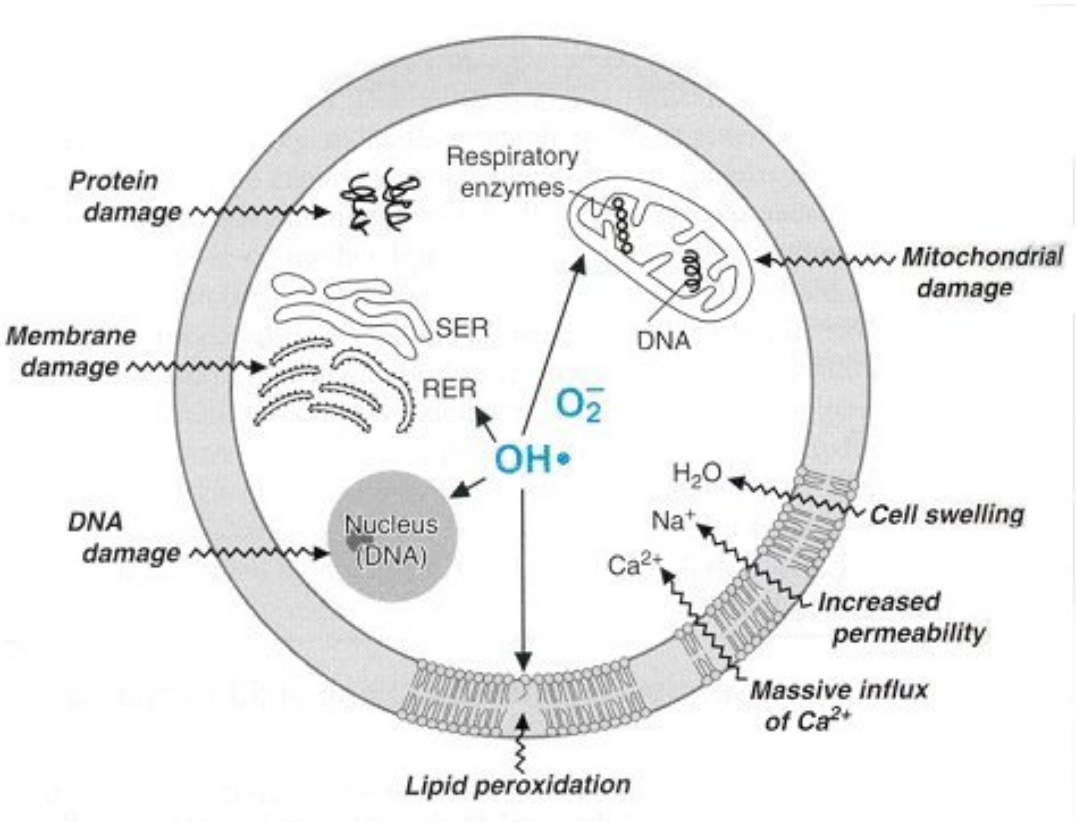

Figure 3.3 Free radical effects on the cell [33].

Hazards of free radicals in cells and tissues can be listed as follows:

a. DNA damage
b. Disintegration of coenzymes with nucleotid structure
c. Breakdown of the structure and functions of enzymes that are depent on thiols, change in the thiol/sulphide ratio of the cell environment
d. Formation covalent bond with lipids and proteins
e. Changes in enzyme activities and lipid metabolism
f. Breakdown of mucopolysakkarides
g. Damage of proteins and increase in protein turnover
h. Lipid peroxidation, change of membrane structure and function
i. Damage of cell proteins, failure in transport mechanisms
j. Aggregation of seroid and age pigments
k. Aterofibrotic changes in capillaries as a result of failure in oxido-reduction reactions in collagen and elastin.

3.2 Lipid Peroxidation

Mammalian cell membranes consists of large amounts of polyunsaturated fatty acids (PUFA) which are very sensitive to peroxidative damage. Peroxidation of these fatty acids, which develops as a chain reaction, is the most important cause of cellular damage.

Radical that combines with the fatty acid starts a series of reactions. Firstly, lipid peroxide radical (ROO·) is formed after fatty acid radical combines with oxygen. Lipid peroxide radicals forms hydroperoxides when they interact with fatty acid side chains. By contribution from some metal ions, these peroxide species react and as a result ethane, pentane and malondialdehyde are formed as break-up products. There are also byproducts which have chemiluminescence and flourescence properties. Due to lipid peroxidation and oxidation of proteins that comprise sulphur, permeability and vulnerablity of the membrane increase and enzymatic activities decreases. This causes the intake of Ca^{+2} to increase. As the intracellular Ca^{+2} concentration increases phospholipase acitivity also increases and phospholipid level decreases. Protease activation, proteolytic effect, activity of catabolic enzymes and endonuclease activity all increase and DNA strand breaks occur.

Free radicals and malondialdehyde react with DNA in the cell membrane. They cause change in chromosal structure and finally cytotoxicity because of base changes in nucleic acid structure and DNA breaks. These reactions result in mutagenic and carcinogenic effects. Many diseases are related to these effects of free radicals in the cell. [12, 13, 14, 33]

Lipid peroxidation ends up with the transformation of lipid hydroperxyls to aldehyde and carbonyl compunds. Amount of one of these compounds, malondialdehyde (MDA), is measured using the thiobarbituric acid test and this method is widely used for determination of lipid peroxidation levels.

Lipid peroxidation causes cellular damage in three ways:

a. Failure in cell functioning
b. Effect of radicals to enzymes and cellular elements
c. Cytotoxic effect of aldehydes

Lipid peroxidation follows a series of reactions, which is shown in a simplified form below:

$LH + R\cdot \rightarrow L\cdot + RH$

$L\cdot + O_2 \rightarrow LOO\cdot$

$LOO\cdot + LH \rightarrow LOOH + L\cdot$

$LOOH \rightarrow LO\cdot + LOO\cdot$ + aldehydes.

3.3 Antioxidant Defense Mechanism

In order to overcome hazardous effects of free radicals there are antioxidant defense mechanisms in the living organisms. Antioxidants get their name because they combat oxidation. They are substances that protect other chemicals of the body from damaging oxidation reactions by reacting with free radicals and other reactive oxygen species within the body, hence hindering the process of oxidation. During this reaction the antioxidant sacrifices itself by becoming oxidized. However, antioxidant supply is not unlimited as one antioxidant molecule can only react with a single free radical. Therefore, there is a constant need to replenish antioxidant resources, whether endogenously or through supplementation.

The word "antioxidant" means different things to different people. Often the term is implicitly restricted to chain-breaking inhibitors of lipid peroxidation. However, free radicals generated in vivo damage many other targets, including proteins, DNA and small molecules. Hence, a broader definition of an antioxidant is "*any substance that, when present at low concentrations compared with those of an oxidizable substrate, significantly delays or prevents oxidation of that substrate*". The term "oxidizable substrate" includes every type of molecule found in vivo. This definition emphasizes the importance of the damage target studied and the source of reactive oxygen species used when antioxidant action is examined in vitro [38].

Types of effects of antioxidants are:

1. Scavenging of reactive oxygen species directly or through enzymatic reactions
2. Preclusion of reactive oxygen species formation by suppression
3. Binding of metal ions, thus preclusion of radical formation reactions
4. Repair and cleaning of target molecules after damage [39].

It is perfectly possible for an antioxidant to protect in one system but to fail to protect, or even sometimes cause damage, in others. Antioxidant inhibitors of lipid peroxidation may not protect other targets (such as DNA and protein) against damage, and sometimes can even aggravate such damage [40].

Antioxidants can be classified according to different criteria:

1. Structure
   a. Enzymes
   b. Non-enzymatic proteins, small molecules
2. Source
   a. Endogenous antioxidants
   b. Exogenous antioxidants
3. Solubility
   a. Soluble in water
   b. Soluble in lipids
4. Location
   a. Intracellular
   b. Plasma and extracellular fluids [39].

The enzymatic and nonenzymatic antioxidant systems are intimately linked to one another and appear to interact with one another. Both vitamin C and GSH have been implicated in the recycling of alpha-tocopherol radicals. (Figure 3.4) [34].

3.3.1 Enzymatic Antioxidants

Although there is quite a large number of enzymatic antioxidants known, we will focus on superoxide dismutase (SOD), catalase (CAT), glutathione peroxidase (GSH-Px). A more simplified form of Figure 3.3 and Figure 3.4 is given in Figure 3.5.

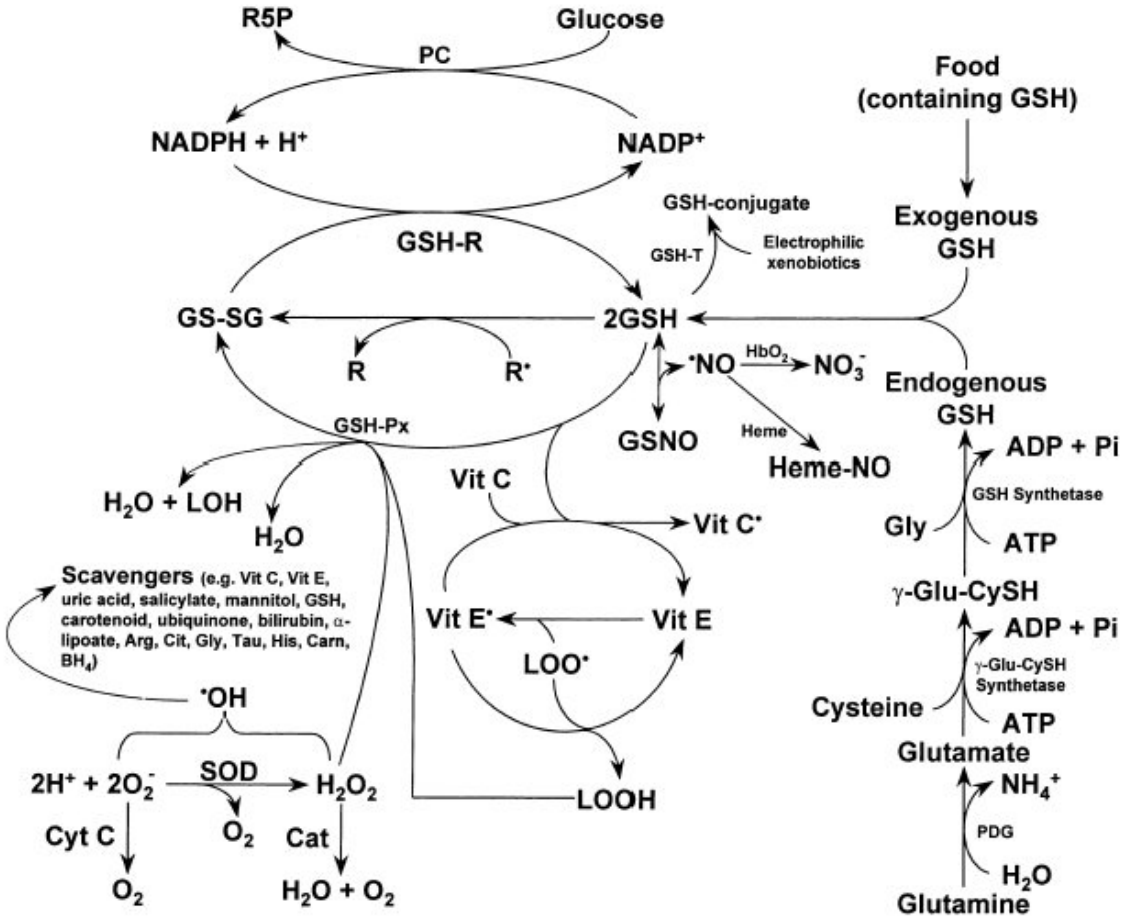

Figure 3.4 Removal of oxygen and nitrogen free radicals and other reactive species in mammalian cells. ADP, adenosine diphosphate; Arg, arginine; BH4, (6R)-5,6,7,8,-tetrahydro-L-biopterin; Carn, carnosine; Cat, catalase; Cit, citrulline; Cyt C, cytochrome C; ETS, electron transport system; Glu, L-glutamate; Gly, glycine; _-Glu-CySH, _-glutamyl-cysteine; GS-SG, oxidized glutathione (glutathione disulfide); GSH, glutathione (reduced form); GSH-Px, glutathione peroxidases; GSH-R, glutathione reductase; GSH-T, glutathione S-transferase; GSNO, nitrosylated glutathione; HbO_2, oxyhemoglobin; Heme-NO, heme-nitric oxide; His, histidine; LOH, lipid alcohol; LOO•, lipid peroxyl radical; LOOH, lipid hydroperoxide; •NO, nitric oxide; NO_3^-, nitrate; O_2^-, superoxide anion radical; $ONOO^-$, peroxynitrite; PC, pentose cycle; R•, radicals; R, non-radicals; R5P, ribulose 5-phosphate; SOD, superoxide dismutase; Tau, taurine; Vit C, vitamin C (ascorbic acid); Vit C•, vitamin C radical; Vit E, vitamin E (α -tocopherol); Vit E•, vitamin E radical [34].

3.3.1.1. Superoxide Dismutase. SOD is an endogenously produced intracellular enzyme present in essentially every cell in the body. Superoxide dismutase (SOD) enzyme catalyzes the following reaction and causes the superoxide radical to transform to hydrogen peroxide and water [41]. Thus superoxide radical levels inside the cell decreases.

$$2\ O_2{\cdot}^- + 2\ H^+ \rightarrow H_2O_2 + O_2$$

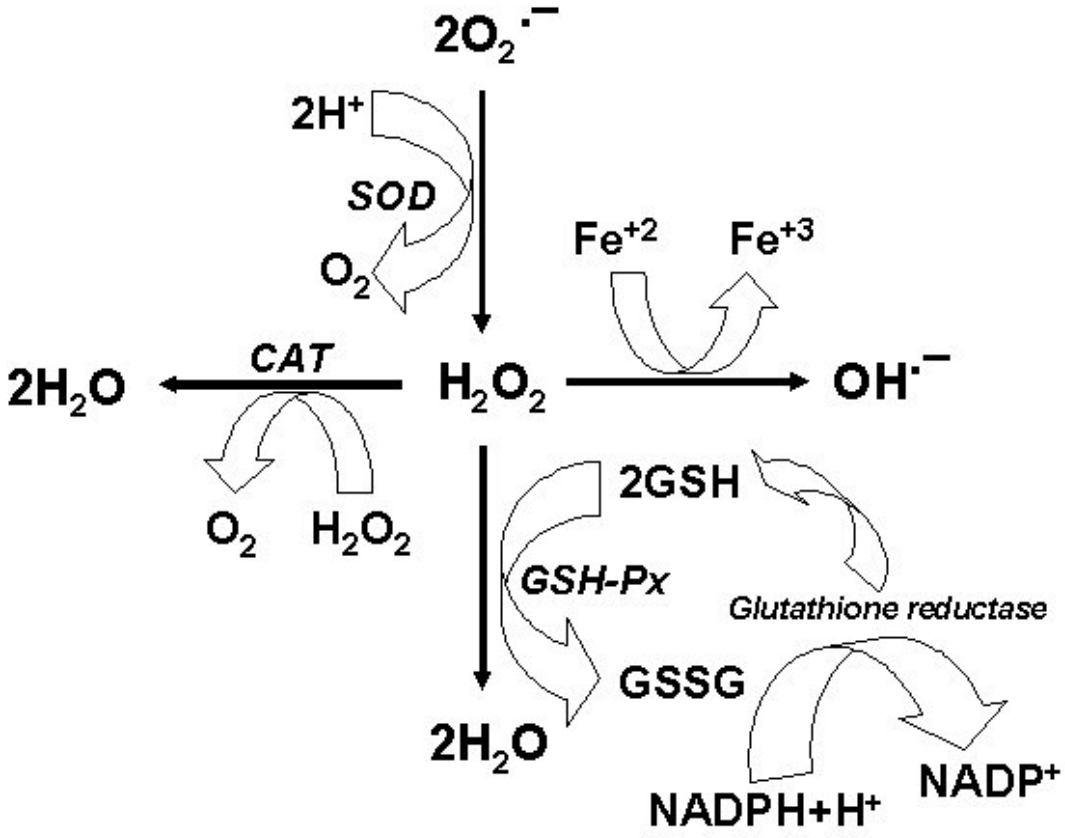

Figure 3.5 Antioxidant defense mechanism.

There are two isoenzymes of SOD in human beings: CuZnSOD and MnSOD. CuZnSOD comprises copper and zinc atoms and is located in the cytosole. MnSOD, on the other hand, is in the tetrameric structure and is located in the mitochondria. CuZn is inhibited by the cyanide while there is no effect of cyanide on MnSOD. SOD activity is high in the tissues that have high oxygen consumption. SOD activity is low in extracellular fluids [39].

The respective enzymes that interact with superoxide and H_2O_2 are tightly regulated through a feedback system. Excessive superoxide inhibits glutathione peroxidase and catalase to modulate the equation from H_2O_2 to H_2O. Likewise, increased H_2O_2 slowly inactivates CuZn-SOD. Meanwhile, catalase and glutathione peroxidase, by reducing H_2O_2, conserve SOD; and SOD, by reducing superoxide, conserves catalases and glutathione peroxidase. Through this feedback system, steady low levels of SOD, glutathione peroxidase, and catalase, as well as superoxide and H_2O_2 are maintained, which keeps the entire system in a fully functioning state.

SOD also exhibits antioxidant activity by reducing $O_2\cdot^-$ that would otherwise lead to the reduction of Fe^{3+} to Fe^{2+} and thereby promote $OH\cdot$ formation. When the catalase activity is insufficient to metabolize the H_2O_2 produced, SOD will increase the tissue oxidant activity. Hence, it was found that the antioxidant enzymes function as a tightly balanced system, any disruption of this system would lead to promotion of oxidation.

3.3.1.2. Catalase. This enzyme is a protein enzyme present in most aerobic cells in animal tissues. Catalase (CAT) is present in all body organs being especially concentrated in the liver and erythrocytes. Catalase catalyzes the reaction that breaks hydrogen peroxide into oxygen and water:

$$2\ H_2O_2 \rightarrow 2\ H_2O + O_2$$

This enzyme, located in peroxysomes, consists of 4 heme groups in its structure. It also has peroxidase activity. While it affects small molecules like hydrogen peroxide and methyl hydroperoxide, it has no effect on lipid hydroperoxides.

Catalase and glutathione peroxidase seek out hydrogen peroxide and convert it to water and diatomic oxygen. An increase in the production of SOD without a subsequent elevation of catalase or glutathione peroxidase leads to the accumulation of hydrogen peroxide, which gets converted into the hydroxyl radical.

3.3.1.3. Glutathione Peroxidase. Glutathione peroxidase (GSH-Px) is located in the cytosole. It is in tetrameric structure and consists of 4 selenium atom. GSH-Px reduces the hydrogen peroxide and hydroperoxides (ROOH) in the following reactions:

$$H_2O_2 + 2\ GSH \rightarrow GSSG + 2\ H_2O$$
$$ROOH + 2\ GSH \rightarrow GSSG + ROH + H_2O$$

There are two substrates of GSH-Px. While one of the substrates, peroxides, reduces to alcohols the other substrate, reduced glutathione (GSH), is oxidized. Oxidized glutathione (GSSG) transforms into reduced glutathione in a reaction that is catalyzed by glutathione reductase enzyme.

$$GSSG + NADPH + H^+ \rightarrow \quad 2\ GSH + NADP^+$$

Another GSH-Px type is called “phospholipid-hydroperoxide glutathione peroxidase”, which contains selenium but is in monomeric structure. It reduces phospholipid-hydroperoxides in the membrane structure to alcohols in the absence of vitamin E and protects the cell against peroxidation.

$$H_2O_2 + 2\ GSH \rightarrow GSSG + 2\ H_2O$$
$$ROOH + 2\ GSH \rightarrow GSSG + ROH + H_2O$$
$$PL\text{-}OOH + 2\ GSH \rightarrow GSSG + PL\text{-}OH + H_2O$$

Other important enzymes in the antioxidant defense system are the glutathione transferase and glutathione reductase.

3.3.2 Small Molecules

Glutathione, ascorbic acid (vitamin C), vitamin E, carotenoids and retinoids, ubikinons, flavonoids, melatonin, uric acid and albumin are the main non-enzymatic small molecules that have antioxidant effect. But we will investigate only glutathione in detail.

3.3.2.1 Glutathione. Glutathione (GSH) is found in high concentrations in many tissues. The majority of GSH is synthesized in the liver, and approximately 40% is secreted in the spleen. It is a tripeptide which can be synthesized from glutamate, cysteine and glisin. It is soluble in water and it is an important reducing agent. It has many metabolic functions. It is the substrate or co-substrate of enzymes like GSH peroxidase, GSH reductase and GSH transferase. Glutathione reacts with free radicals and peroxidases and protects the cells from oxidative damage. In addition, it keeps the sulphydryle (-SH) groups of the proteins in reduced state and precludes the inactivation of many proteins and enzymes. It helps the transportation of amino acids through the membrane. Reduced glutathione (GSH) is oxidized in some reactions and transforms into oxidized glutathione (GSSG). GSSG is further reduced in a reaction that uses NADPH. Thus GSH/GSSG ratio in tissues is kept in high levels (>100:1) [39].

The detoxification capability of GSH is directly related to its reduced thiol group. The enzymatic activity of glutathione-peroxidases and glutathione-transferases is also dependent on reduced thiol group of GSH. GSH and other reduced thiols are important for the ability of the body to resist oxidant stress. It has been postulated that decreased levels of reduced GSH would be a marker for increased susceptibility to oxidant injury and also indicating depletion of reserves due to oxidative stress [42].

A decrease in GSH is a risk factor for chronic diseases that may be used to monitor the severity and progress of the diseases. Glutathione decreases have been associated with a variety of diseases such as sepsis, adult respiratory distress syndrome, diabetes mellitus, liver disease, AIDS, and cataracts. Normal blood GSH concentrations occur in healthy adults and decreased GSH levels are found in the elderly and in those with chronic diseases [43].

4. EXPERIMENTAL SETUP AND DOSIMETRY

In this chapter, we will investigate how the experimental setup is designed, how the dosimetry assessment is performed and how other parameters related to the exposure are determined.

4.1 Exposure Environment and Electromagnetic Field Application

The test setup is a general purpose electromagnetic shielded chamber that is suitable to house laboratory animals. In this exposure environment, electromagnetic radiation of specific energy, frequency and waveform can be applied. The main element of the setup is a GTEM Cell [GTEM 1750, MEB Mess Elektronik Berlin], installed in EMC TEMPEST Test Center at TÜBİTAK-UEKAE, Gebze, Kocaeli (see Figure 4.1 and Figure 4.2).

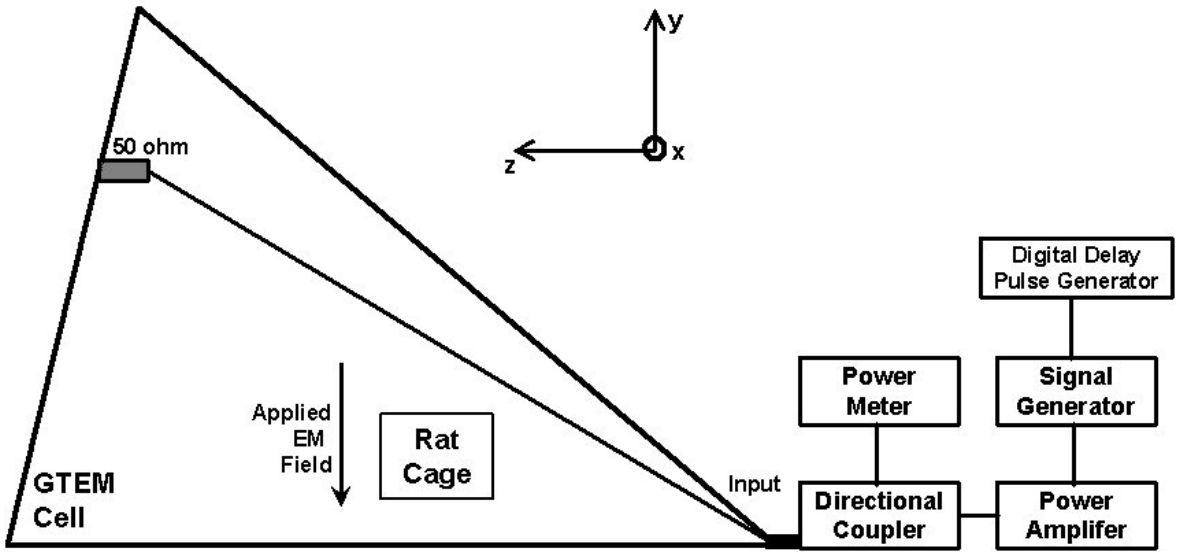

Figure 4.1 Experimental setup for the investigation of biological effects of electromagnetic fields.

Figure 4.2 The GTEM Cell.

GTEM Cell is a radiated field generation and measurement device that has a single input/output port for EM immunity and emission test purposes. GTEM Cell, in essence, is a transmission line terminated with 50 Ω load. The asymmetrical inner conductor (called "septum") is designed to match the impedance of a tapered, rectangular wave guide cross section. The outer surface of the GTEM Cell is made of metal sheets with an attenuation of around 60 dB at high frequency EM fields. Note that honeycomb waveguides are installed at the bottom of the GTEM Cell for ventilation purposes. Electric field level is directly proportional to the amplitude of the voltage applied to the input port and inversely proportional with the septum height. In order to obtain increased field level with constant input power, cages that contain the test subjects are placed closer to the input port of the GTEM Cell for the purpose of biological effect studies.

The rats are enclosed inside two "*metabolic cages*" which are placed adjacent to each other. These cages are designed so as to feed and water the rats and collect urine samples through its structure. The cages are composed of transparent Plexiglas material. It is thus assumed that the cages have minimal effect on the applied electric field. The rats are free to move inside a volume of 24 cm (W) x 34 cm (L) x 12.5 cm (H). The applied electric field is perpendicular to the plane on which the rats move; therefore each animal is exposed to the field without any obstruction caused by its "neighbors".

4.1.1 Generation and Verification of GSM Signal

Let us remember some characteristics of GSM digital mobile communication system. Frequency band is 890 MHz – 960 MHz, in general. But base transceiver station (BTS) downlink frequency band is 935 – 960 MHz. Frame duration is 4.615 ms and timeslot duration is 0.577 μs. This reduces the average power to one-eighth. Modulation technique is GMSK (Gaussian Minimum Shift Keying) and this produces a data rate of 270.833 kbits/s but no significant change in the amplitude. So GSM signal is simulated in the laboratory environment using these characteristics.

GSM modulated signal is generated by using Rohde & Schwarz SMY01 (9 kHz – 1 GHz) signal generator and Stanford Research Systems DG535 Digital Delay/Pulse Generator. SMY01 provides the carrier wave at 945 MHz (which is inside the 935 – 960 MHz band) and DG535 provides the pulse modulation with pulse period 4.615 ms and pulse width 0.577 μs. This corresponds to a rate of 217 Hz with 1/8 duty-cycle.

Generated GSM signal is verified using Agilent Technologies Infinium 54835A (4 GSa/s) oscilloscope. The resultant waveform is shown in Figure 4.3 to help visualization.

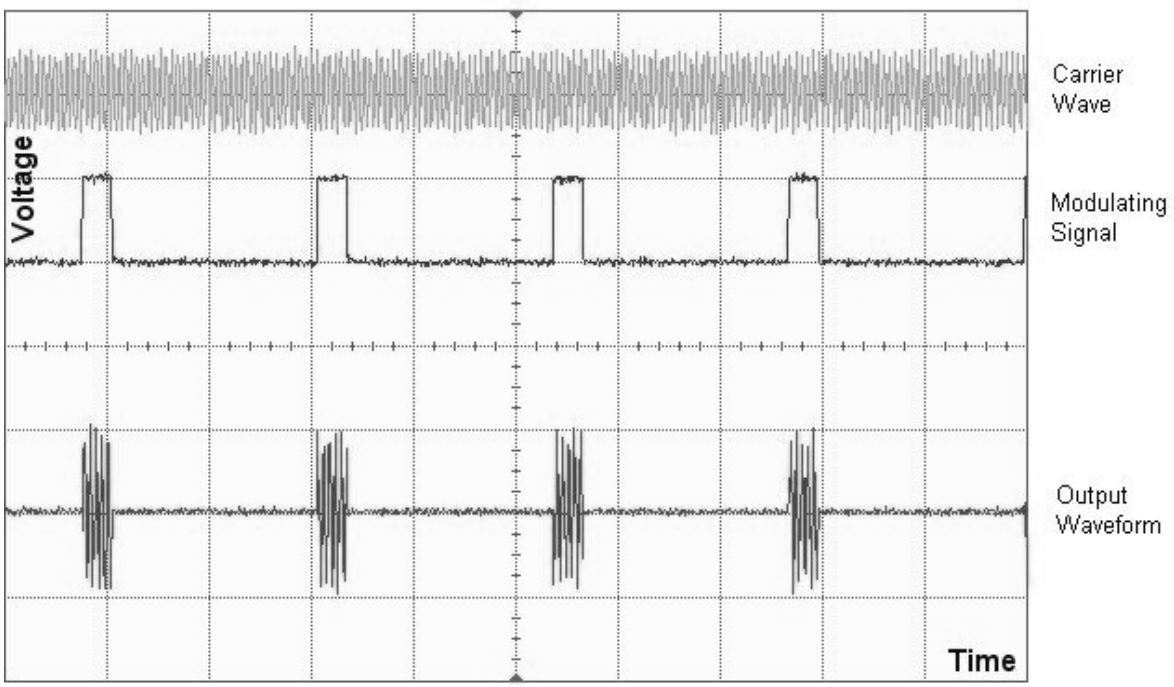

Figure 4.3 Generation of GSM signal.

4.1.2 Application of GSM Signal in the GTEM

Generated GSM signal is then applied to the input of the GTEM cell after it is amplified by Kalmus 757LCB-CE (100 W) amplifier. Input power is measured using the output of directional coupler and directing it to Rohde & Schwarz NRVS Power Meter with NRV-Z51 thermal probe. Directional coupler is placed before the GTEM input. While applied signal travels from the input port of the coupler to the output of it, a third port of it gives 40 dB lower output than the applied signal. So we can have an idea of the applied power without any reference to the amplifier gain.

4.2 SAR Calculation

It is necessary to make the dosimetric evaluation of an electromagnetic field exposure experiment in order to deduce meaningful results and compare various biological effects observed using different test setups. Dosimetric evaluation is performed, in general, in terms of Specific Absorption Rate, known as “SAR” in short. Basic information regarding SAR is given in Appendix B.

Since exposure from Base Transceiver Stations (BTS) is generally in the far field, whole-body average SAR is taken into consideration in this experiment. Whole-body average SAR is defined as the total energy, transferred to the body per unit time, divided by the total mass.

The Finite-Difference Time-Domain (FDTD) method implemented in a MATLAB program [The MathWorks Inc.] was used to compute the expected SAR values on the subjects in a simulation environment [44].

Before FDTD method was implemented to have the dosimetric evaluation of the exposure setup, a few alternative methods have also been experimented. First, dosimetric evaluation was performed by thermometric method and then by using a computer simulation implementing Finite Element Method (FEM). The first two methods did not produce satisfactory results, so finally FDTD method was applied. All three methods and their results are explained below.

4.2.1 Thermometric Dosimetry

Dosimetric evaluation of the test setup by temperature measurement was performed on three sessions with valuable contributions by Prof.Dr. Tunaya Kalkan from İ.Ü. Cerrahpaşa Medical Faculty. Exposure setup used for thermometric dosimetry evaluation is given in Figure 4.4.

Luxtron 3100 Fluoroptic Thermometer [Luxtron Corp.] was used for temperature measurements. Sensors have been placed in rectal, brain, subcutaneous and intraperitonel regions of the rat. Connecting fiber optic cable has been taken out of through ventillation holes installed at the floor of the test chamber. The fluoroptic thermometer was left outside the GTEM Cell. Data acquisition was performed by a personal computer over serial interface via communications software. The sleep or wakefulness of the rat was checked time by time during experiments.

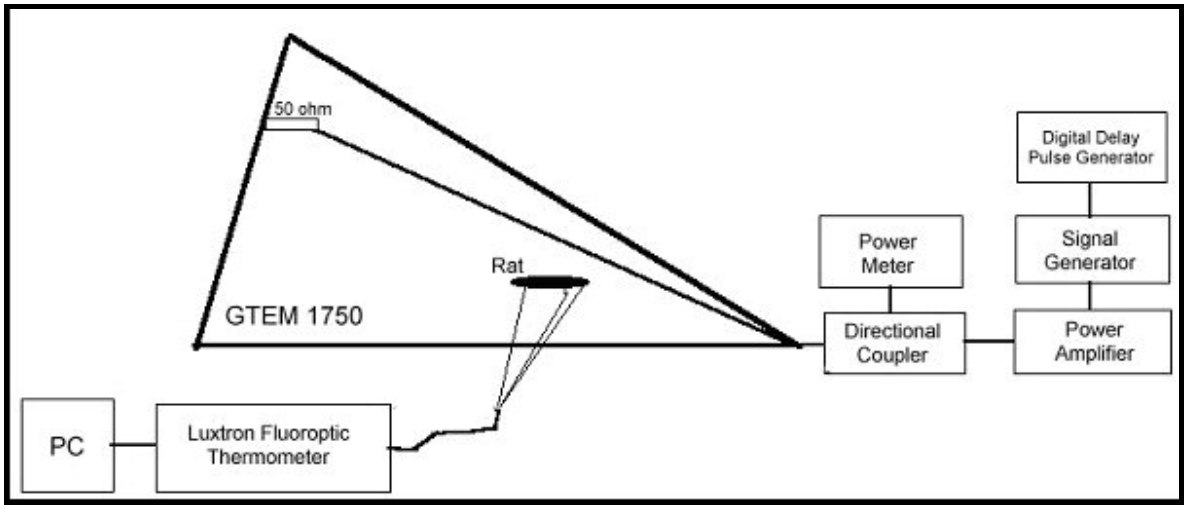

Figure 4.4 Thermometric dosimetry measurement in GTEM Cell.

The rat under exposure was placed to a close point near the apex of the GTEM cell just as planned for the actual test. The septum height at that point was 75 cm. Specification of the height is important because electric field that the rat is exposed to is inversely proportional to the septum height.

Signal generator provided either a GSM modulated signal (when the Digital Delay/Pulse Generator was active) or a continuous wave (CW). Signal level was amplified using Amplifier Research (50 W) or Kalmus (100 W) amplifiers. Electric field levels were

calculated using the Power Meter which provides data on input power levels. Electric field measurements were also performed using EMR-300 Electromagnetic Radiation Meter and its associated probe.

Two Wistar albino rats were used in three different steps at in the thermometric evaluation. In the first and second step, the first and second rats, respectively, were anesthetized and temperature measurements were performed with different input power levels. In the third step, electric fields were applied to the cadaver of the first rat.

The results of the measurements on the first rat, both for the anesthetized and cadaver form, are given in the Figure 4.5 through Figure 4.8. The results are also summarized in Table 4.1 and Table 4.2.

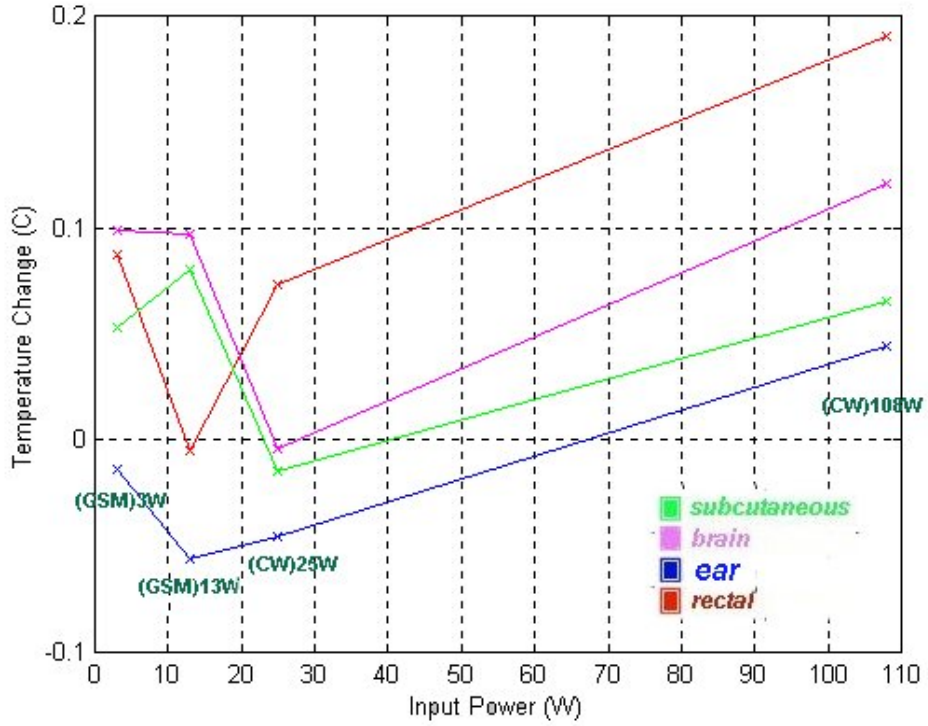

Figure 4.5 Results of temperature measurements for the anesthetized rat after 1 minute of exposure at different power levels and modulation types.

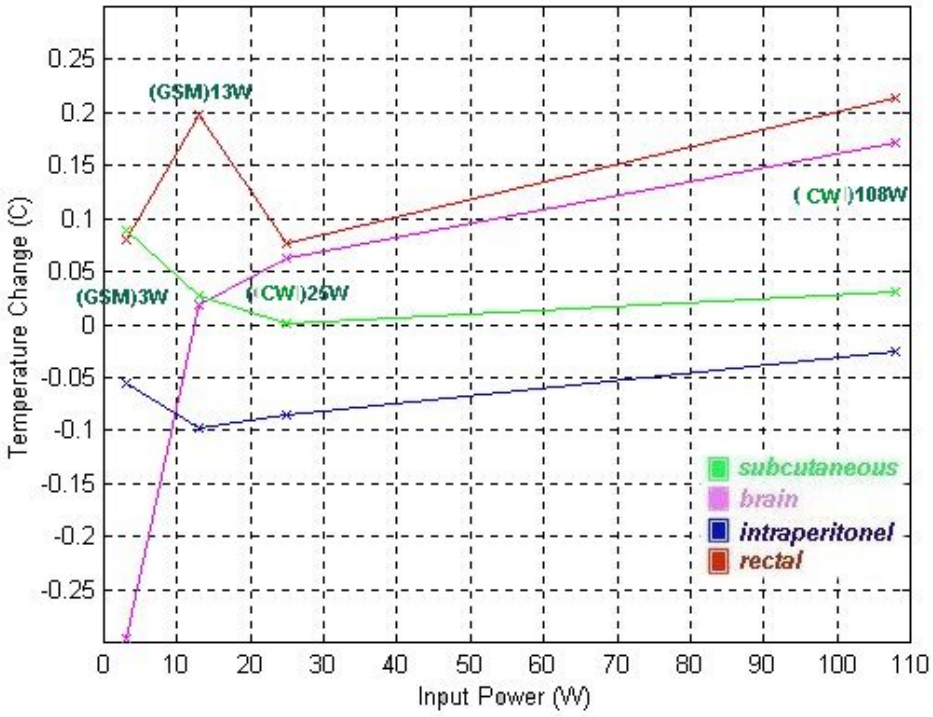

Figure 4.6 Results of temperature measurements for the anesthetized rat after 2 minutes of exposure at different power levels and modulation types.

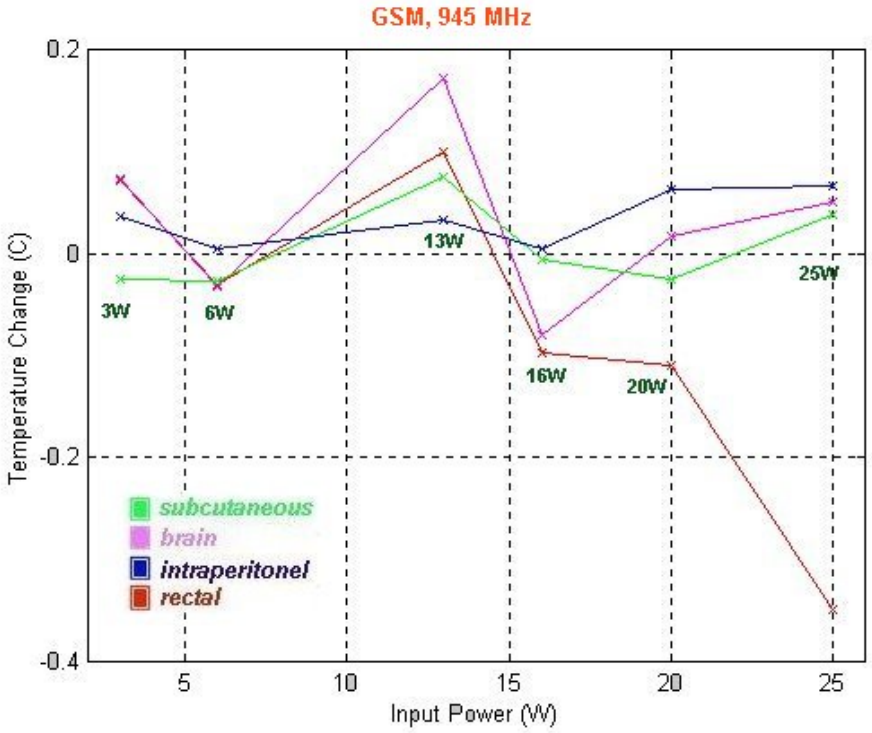

Figure 4.7 Results of temperature measurements for the rat cadaver after 1 minute of 945 MHz GSM exposure at different power levels.

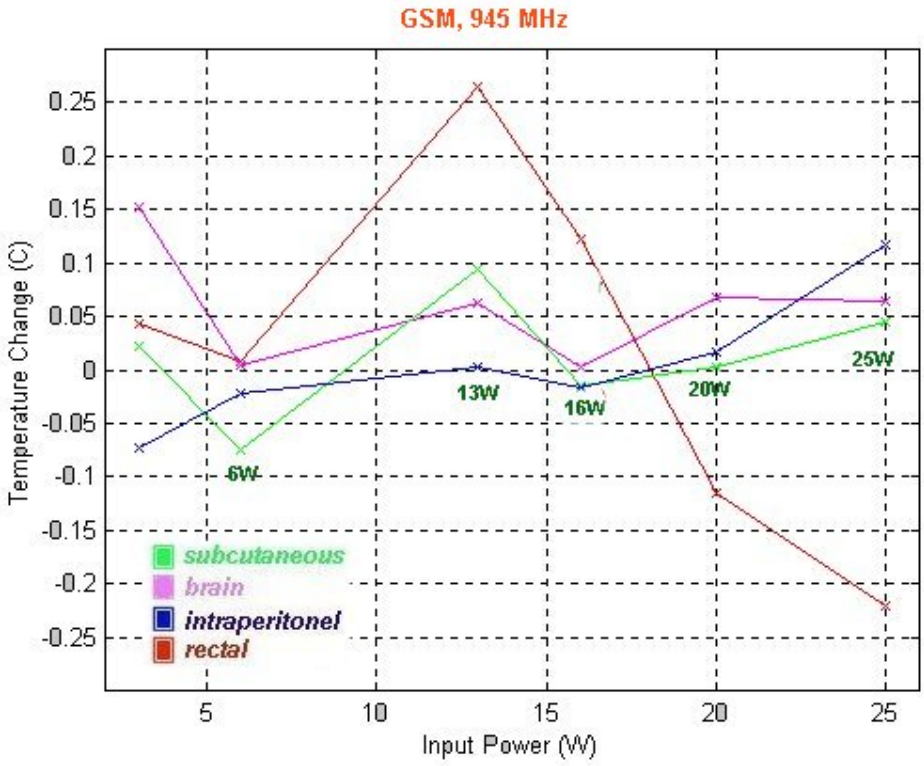

Figure 4.8 Results of temperature measurements for the rat cadaver after 2 minute of 945 MHz GSM exposure at different power levels.

Table 4.1 Temperature increase in the brain of an anesthetized rat after exposure to electromagnetic fields for 2 min and the associated SAR values.

Frequency (MHz)	Modulation	Applied Power (W)	Temperature Difference (^{o}C)	SAR (W/kg)
945	GSM	13	0.0192	0.56
945	CW	108	0.1717	5.03
950	GSM	12	0.0317	0.93
950	CW	96	0.1125	3.30

Table 4.2 Temperature increase in brain of a rat cadaver after exposure to electromagnetic fields for 2 min and the associated SAR values.

Frequency (MHz)	Modulation	Applied Power (W)	Temperature Difference (^{o}C)	SAR (W/kg)
945	GSM	6	0.0050	0.15
945	GSM	13	0.0625	1.83
945	GSM	16	0.0025	0.07
945	GSM	20	0.0675	1.98
945	GSM	25	0.0650	1.90
945	CW	108	0.1275	3.74

SAR values calculated according to temperature increase in anesthetized and cadaver rat bodies due to exposure to electromagnetic fields generated inside the GTEM Cell does not show a reasonable correlation with the power applied to the input port of the GTEM Cell.

Main reason for this may be that the level of the electromagnetic field was not enough to cause any increase in temperature. Another reason may be that the temperature resolution of the measurement probes, which is 0.01 ^{o}C, was not enough to measure small increases in the temperature. In addition, temperature variations as a result of thermal regulation in anesthetized rats might have masked the temperature variations due to electromagnetic field exposure. It was not possible to apply higher power levels because of the restrictions associated with the power amplifier. Therefore, there seems to be no conclusive correlation between the applied power levels and the SAR values.

4.2.2 Computer Simulation Using Finite Element Method

Determination of experimental dosimetry by the Finite Element Method (FEM) method was also studied using Agilent High Frequency Structure Simulator (HFSS) Release 5.5 software which is based on this method.

Since the dimensions of the GTEM cell is too large when compared to the size of the rat, GTEM cell was not simulated in full. Rather only the portion where the rat is placed was simulated. Several trial runs have been performed in order to reach an optimal problem description. An example for the model that is used in trial runs is given in Figure 4.9. An example of the numerous outcomes of the simulation is given in Figure 4.10. Here shades of color represent different electric field levels.

Note that some approximations have been applied when modeling the exposure environment. This brought some deficiency in the results. What we obtained from the HFSS FEM modeling was only some qualitative idea that electric field inside rat tissue is small compared to the surrounding air medium.

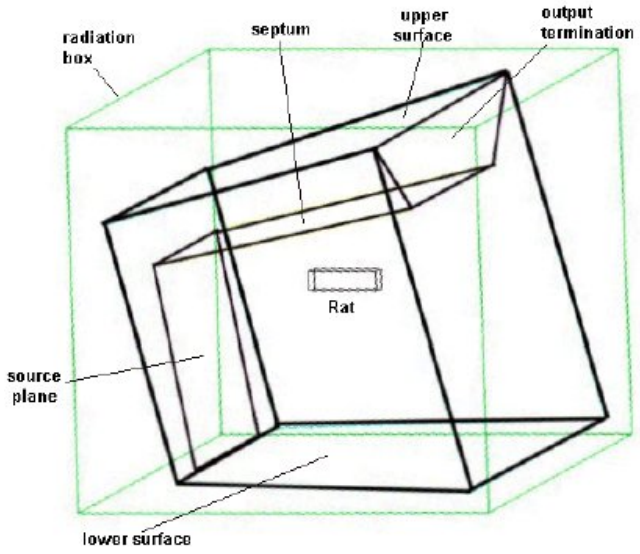

Figure 4.9. Model of the GTEM Cell and the Rat Used for the HFSS Simulation.

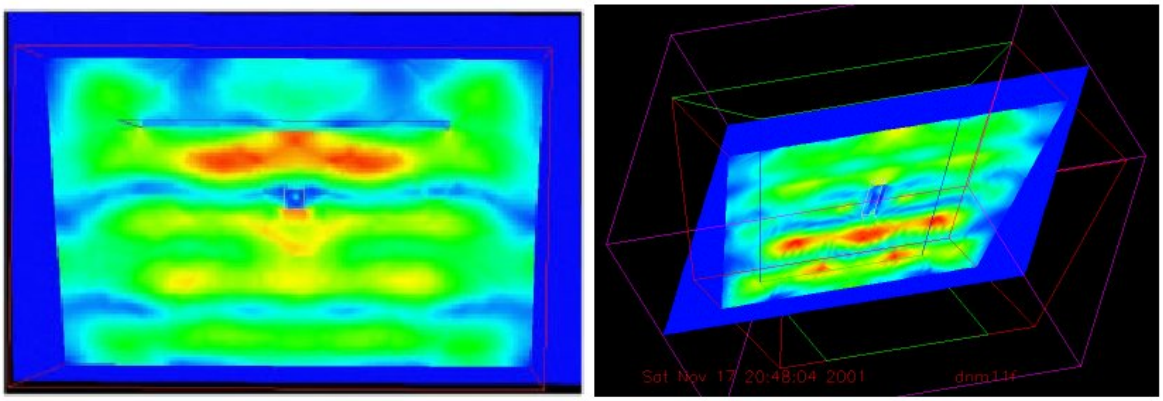

Figure 4.10. Graphical representation of the outcome of the HFSS simulation for (a) xy-plane and (b) xz-plane.

4.2.3 The Finite Difference Time Domain Method

The finite-difference time-domain (FDTD) method belongs to the general class of differential time domain numerical modeling methods. FDTD concept was first introduced by Yee in 1966. This technique involves the discretization of the differential form of Maxwell's equations in time and space using second-order accurate central differences. The resulting difference equations are then solved in a time marching sequence by alternately calculating the electric and magnetic fields on an interlaced Cartesian grid [27].

When modeling the GTEM Cell for the FDTD technique, only the region where the test subject is present was considered due to the demanding computation duration and complexity (Figure 4.11). The test subject was, on the other hand, modeled roughly as shown in Figure 4.12, trying to maintain some details of its geometry. The rat was modeled using electrical properties calculated for average muscle at 945 MHz, i.e. ε=55.853462, σ=0.985515. The density of the rat tissue was taken as ρ=1040 mg/cm^3.

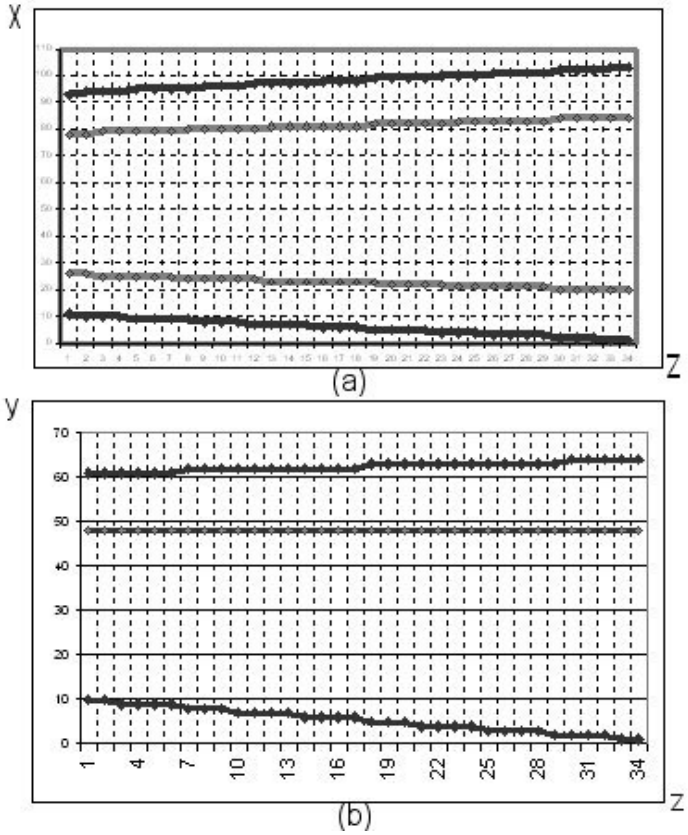

Figure 4.11. Cross-sections of the model of the GTEM Cell (a) in XZ plane and (b) in YZ plane developed for FDTD technique.

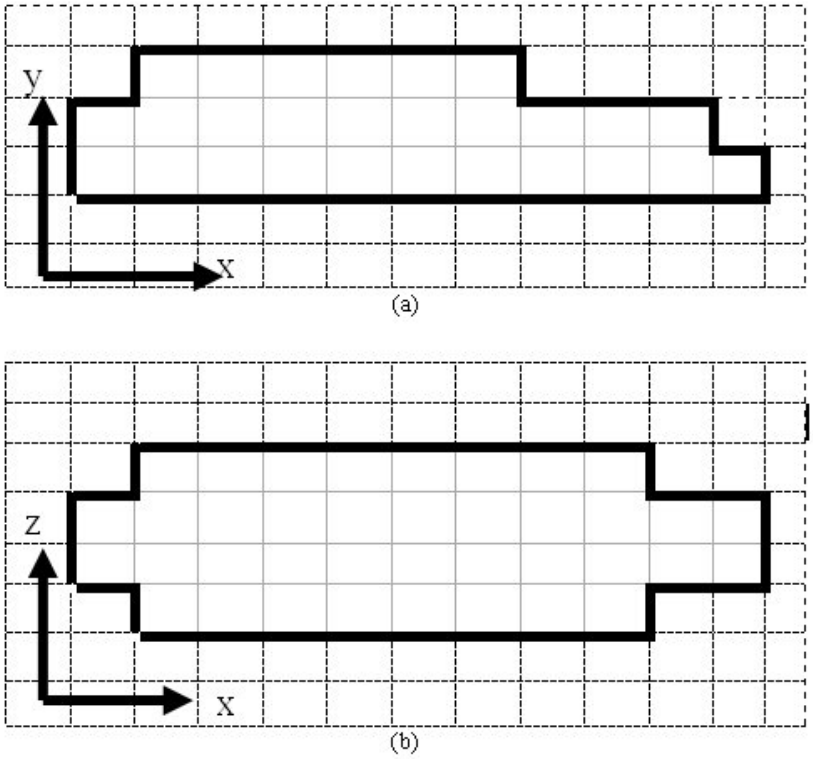

Figure 4.12. Cross-sections of the model of the test subject (a) in XY plane and (b) in XZ plane developed for use in the FDTD technique.

4.2.3.1 Verification of the FDTD Modeling. In order to verify that FDTD numerical modeling was successfully applied to the problem, the results of the model were compared with the results of actual electric field measurements. The FDTD modeling program was run in order to find electric field levels at 10 selected positions on an XY plane located at the middle point of the Z axis (see Figure 4.13). These points were selected such that they represent the position of the rats in metabolic cages during actual electromagnetic field exposure. Note that the rats were placed at 50 cm height inside the GTEM cell during the experiment. The program was run for three times for different input power levels, i.e. 10 Watts, 20 Watts and 25 Watts.

Measurements were performed at the same 10 positions by using Acterna (formerly Wandel & Goltermann) electric field meter device EMR-300 with a Type 8 probe (200 kHz – 3 GHz), again at the specified input power levels. The frequency was 945 MHz for all cases. The results of this study are summarized in Table 4.3, Table 4.4 and Table 4.5.

We found out that FDTD model closely simulates the actual exposure environment (less than 7% difference in the average electric field levels). Thus, the model is a good approximation of the real life measurements. Electric field measurement results also indicated that a fairly uniform electric field was applied to the test subjects in the exposure environment.

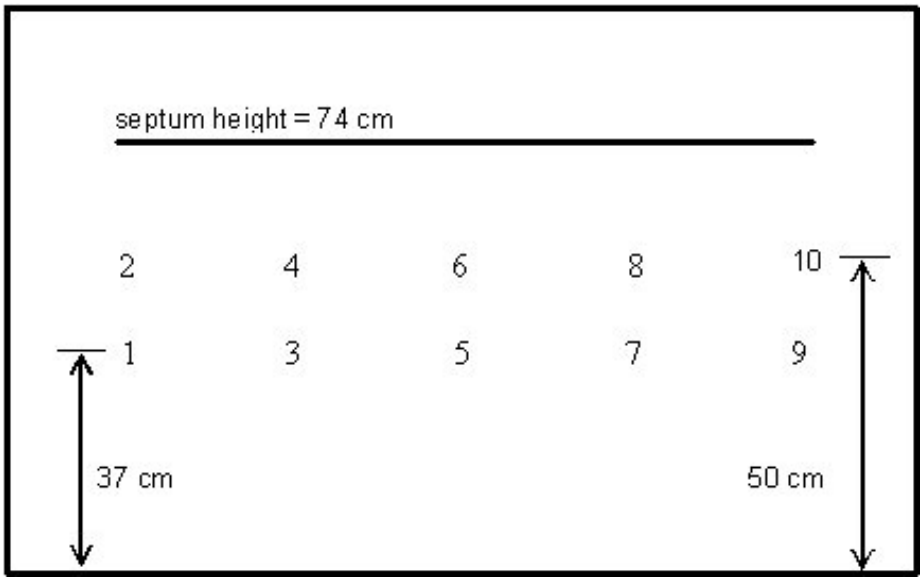

Figure 4.13. Location of the points where the electric field levels are computed numerically and measured analytically.

Table 4.3. Results of comparison study for 10 W input power level.

Position	Measurement (V/m)	Numerical (V/m)	Difference (V/m)	% Difference	dB Difference
1	30.7	26.0	4.7	15.3	1.4
2	39.5	34.8	4.7	11.9	1.1
3	30.9	31.1	0.2	0.6	0.1
4	36.4	37.8	1.4	3.8	0.3
5	30.5	29.2	1.3	4.3	0.4
6	30.9	34.6	3.7	12.0	1.0
7	32.7	31.4	1.3	4.0	0.4
8	37.4	38.0	0.6	1.6	0.1
9	29.4	26.6	2.8	9.5	0.9
10	36.6	35.7	0.9	2.5	0.2
			Average	**6.6**	**0.6**

Table 4.4. Results of comparison study for 20 W input power level.

Position	Measurement (V/m)	Numerical (V/m)	Difference (V/m)	% Difference	dB Difference
1	40.0	36.8	3.2	8.0	0.7
2	55.6	49.3	6.3	11.3	1.0
3	43.7	44.0	0.3	0.7	0.1
4	51.4	53.4	2.0	3.9	0.3
5	43.3	41.2	2.1	4.8	0.4
6	43.7	48.9	5.2	11.9	1.0
7	45.7	44.4	1.3	2.8	0.3
8	52.3	53.7	1.4	2.7	0.2
9	41.8	37.6	4.2	10.0	0.9
10	51.3	50.6	0.7	1.4	0.1
			Average	**5.8**	**0.5**

Table 4.5. Results of comparison study for 25 W input power level.

Position	Measurement (V/m)	Numerical (V/m)	Difference (V/m)	% Difference	dB Difference
1	48.8	41.2	7.6	15.6	1.5
2	61.7	55.1	6.6	10.7	1.0
3	48.6	49.2	0.6	1.2	0.1
4	56.9	59.7	2.8	4.9	0.4
5	48.1	46.1	2.0	4.2	0.4
6	48.6	54.7	6.1	12.6	1.0
7	51.2	49.6	1.6	3.1	0.3
8	58.1	60.0	1.9	3.3	0.3
9	46.7	42.0	4.7	10.1	0.9
10	56.8	56.6	0.2	0.4	0.0
			Average	**6.6**	**0.6**

4.2.3.2 FDTD Modeling Results. Calculated SAR values from various applied power levels for a single rat test model and for a four-rat test model according to equations given in Appendix B are shown in Table 4.6. Four-rat test model was computed in order to see the effects of other test subjects in the test volume since more than one rat would be used in the biological effects experiment. Internal electric field levels computed for three layers of the rat model in the XZ plane for 25 W input power are shown in Figure 4.14. No difference in the results due to modulation scheme (i.e. GSM or CW) was anticipated because the time period where FDTD technique was applied was too short and it covers only the CW segment.

Table 4.6. Whole-body average SAR values computed using the FDTD technique at 945 MHz.

Frequency (MHz)	Applied Power (W)	SAR (W/kg) [Single rat model]	SAR (W/kg) [4 rat model]
945	10	0.0083	0.0089
945	20	0.0166	0.0178
945	25	0.0207	0.0223
945	50	0.0412	0.0446
945	108	0.0895	0.0962

When modeling the exposure setup using the FDTD technique, we could observe a reasonable correlation between the applied power levels and the SAR values although the rat was again modeled roughly. First of all, two dimensional distributions of computed electric field levels in a cross-sectional plane in XY plane is in line with two-dimensional results previously calculated using analytical and numerical methods. When the calculated SAR value is normalized to the applied power level, 8.9×10^{-4} W/kg per input Watt (or 0.89 mW/kg per input W) is obtained. Thus, when this exposure setup is used for assessment of biological effects, we can compute the SAR value easily once the input power level is given.

4.3 Electromagnetic Exposure

Calculations above show that in this test environment SAR values we can induce are well below the safety standards [1, 2, 3]. A set of exposure experiments were performed in two phases to investigate the biological effects of the electromagnetic fields at GSM BTS frequency. The first phase was the EM field exposure experiment and the second was the sham exposure (see Table 4.7). In each phase, the following procedure was applied:

The animals were obtained from the Experiment Animals Center of Istanbul University Cerrahpasa Medical School. For each of the two phases a set of 9 healthy, young adult male Wistar albino rats were used. The rats were cared for in accordance with the Guide for the Care and Use of Laboratory Animals [45]. The rats have been fed with standard pellet food and watered by tap water ad libitum. The rats have been weighted before, after and at each day of the experiment. Average weights of both groups before and after the experiment and their average food and water consumption are given in Table 4.8.

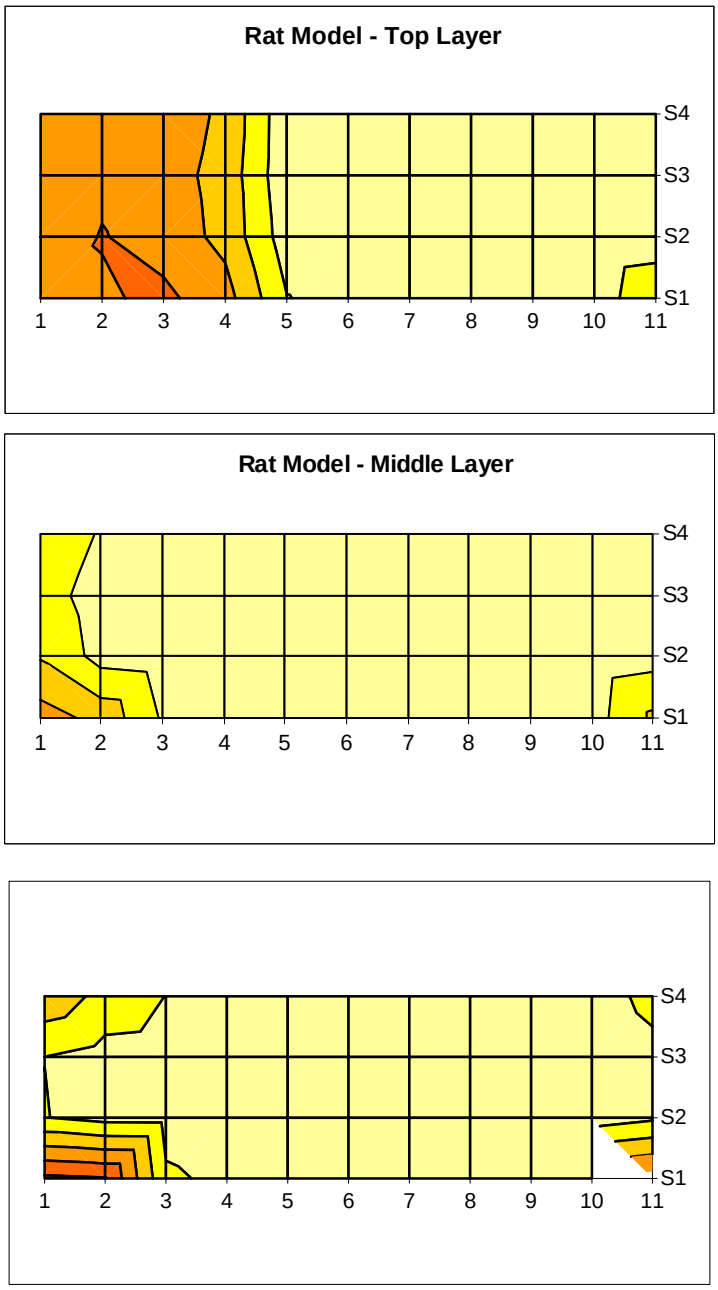

Figure 4.14. Electric field levels (V/m) computed using FDTD technique in the three layers of the rat model in XZ plane for 25 W input power.

Table 4.7. Exposure parameters.

Phase	# Rat	GTEM Input Power (W)	Applied E Field Level (V/m)	Power Density (W/m^2)	SAR (mW/kg)	Exposure Duration (days)	Effective Exposure Time (hours/day)	Time Spent in GTEM Cell (hours/day)
Experiment	9	12.5	37.2	3.67	11.3	8	7	7
Sham Exposure	9	-	-	-	-	8	-	7

Table 4.8. Average weights of the rats before and after the experiment and their average food and water consumption.

Groups of Rats	Initial Weights (g)	Weights After Exposure (g)	Average consumed food per day by single rat (g)	Average consumed water per day by single rat (ml)
Experiment	190 ± 40	220 ± 38	22	21
Sham Exposure	162 ± 43	191 ± 44	30	18

The subjects were placed inside two metabolic cages, 5 rats in one cage and 4 rats in the other. The cages were placed in the test volume inside the GTEM cell as shown in Figure 4.15. Radiofrequency EM field (3.67 W/m^2 power density) was applied onto the exposure group for the first phase, while there was no EM field exposure onto the sham group, in the second phase. We could only apply a low power level, which corresponds to a SAR value of 11.3 mW/kg, because of the time-averaging of the applied peak power level in accordance with the GSM modulation of the carrier wave. The cages containing the rats were kept inside the GTEM Cell for 7 hours for a period of 8 days for each group.

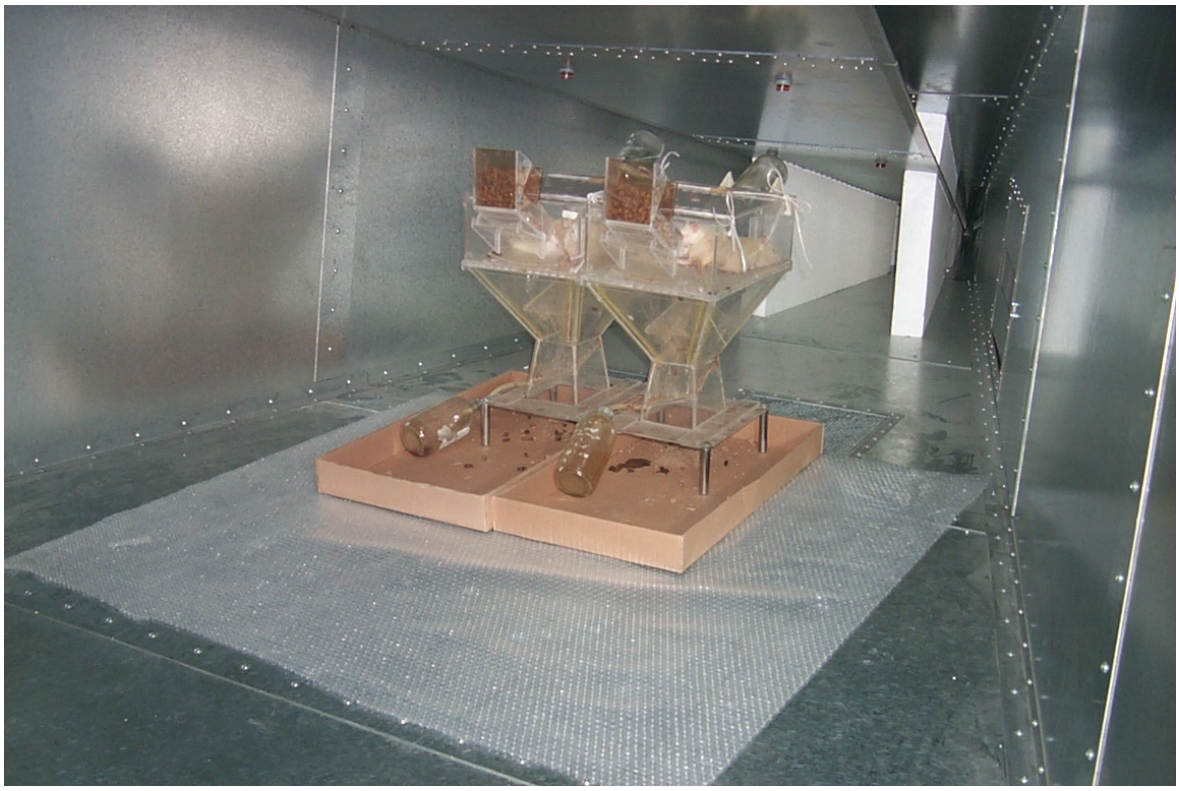

Figure 4.15. A group of rats contained in two metabolic cages inside GTEM Cell.

4.4 Metabolite Gathering and Analysis

Basic biological parameters that are of interest in this thesis study were malondialdehyde (MDA), glutathione (GSH) and superoxide dismutase (SOD) levels which have been determined using biochemical analysis techniques. Leukocyte analysis on blood samples and vanil mandelic acid (VMA) analysis on urine samples have also been performed.

4.4.1 Biochemical Analysis

At the end of each phase, the animals were anesthetized. After exploration of the thorax, intracardiac blood was quickly obtained. The tubes containing the processed blood samples were stored at -24 ^{o}C until they were analyzed at the İ.Ü. Cerrahpaşa Medical School Biochemistry Laboratory. These samples were processed for measuring MDA, GSH and SOD levels. The materials collected were analyzed using a spectrophotometer [JASCO V-530 UV/VIS] according to standard laboratory procedures, as explained in Chapter 5 [46, 47].

4.4.2 Leukocyte Analysis

Leukocyte analysis was performed on blood samples taken from the tail of the rats. A few drops of blood have been obtained from rat tails by a small scratch and have been spread on microscope slides. This action was accomplished two times for each rat at Cerrahpaşa Medical School Biophysics Department before rats have been transferred to and from TÜBİTAK UEKAE EMC Laboratory, i.e. before and after exposure experiment. A collection of blood samples on microscope slides are shown in Figure 4.16. These blood samples have been dried for a few weeks before they have been analyzed at İ.Ü. Cerrahpaşa Medical School Pathology Laboratory.

Figure 4.16 Slides of blood samples for leukocyte count.

4.4.3 Urine Analysis

Vanil mandelic acid, or vanillyl mandelic acid (VMA), is a chemical end product of catecholamine metabolism. It is found in urine together with homovanillic acid (HVA). In timed urine tests its quantity (concentration μg / 24 h) is assessed, along with creatinine clearance, and the concentration of cortisols, catecholamines, and metanephrines. Noradrenaline is released during stressful conditions and metabolized to vanillyl mandelic acid (VMA) peripherally and 3-methoxy 4-hydroxyphenyl glycol centrally. VMA, the major metabolite of sympathetic amines, is taken as indirect biochemical index to represent the increase in peripheral sympathetic activity during stress [48].

Urine samples were collected inside two bottles located at the bottom of each cage. Urine samples travels through metabolic cage structure and ends up at the bottles. Since it was not possible to obtain urine samples from each rat, a total analysis was performed but on time basis, i.e. every two days. Vanil mandelic acid (VMA) levels have been analyzed at İ.Ü. Cerrahpaşa Medical School Central Laboratory.

5. BIOCHEMICAL ANALYSIS METHODS

The focus of this thesis study is the effect of electromagnetic fields on specific biochemical parameters. This chapter gives brief description of the biochemical analysis methods applied for determination of malondialdehyde (MDA), superoxide dismutase (SOD) and glutathione (GSH) levels.

5.1 MDA Determination (TBARS Method)

The principle is the spectrophotometric determination of absorbance at 535 nm of colored complex which is formed by condensation of two molecules of thiobarbituric acid and one molecule of the material that it reacts with.

First the stock solution is prepared with the following concentrations:

Stock solution

Molecule	**Concentration**
Trichlor-acetic acid	15 %
Thiobarbituric acid	0.375 %
Hydrochloric acid	0.25 N

The method is applied as described below:

	Blind (ml)	**Assay (ml)**
Specimen (plasma)	-	0.5
Distilled water	0.5	-
Stock solution	1	1

After pippeting, tubes are closed and put inside a boiling water bath for 20 minutes. After cooling down, they are centrifuged at 2000 cycles/min for 10 minutes. Absorbance of the supernatant solution is read against the blind solution.

For TBARS (thiobarbituric acid reactive substances) molar extinction coefficient is, $\varepsilon = 1.56 \times 10^5 / (M\ cm)$.

Since total volume is 1.5 ml and specimen volume is 0.5 ml,

$$\text{TBARS}\,(\text{mmol} / \text{L}) = \frac{1.5 \text{ x } A_{test}}{0.5 \text{ x } 1.56 \text{ x } 10^5} \qquad (5.1)$$

5.2 Glutathione Determination

Virtually all of the nonprotein sulphydryl groups of red blood cells are in the form of reduced glutathione. The principle of determination is the color reading at 412 nm of the solution that is formed by the reaction of free sulphydryl compounds in the whole blood with 5,5'-Dithiobis (2-nitrobenzoic acid) (DTNB). Note that DTNB is a disulfide chromogen that is readily reduced by sulfhydryl compounds to an intensely yellow compound and the absorbance of the reduced compound is directly proportional to the GSH concentration.

Reagents used in glutathione determination are listed as follows:

Precipitating reagent : 1.67 g glacial metaphosphoric acid, 0.20 g disodium ethylene diamintetra acetic acid (EDTA) and 30 g NaCl is mixed with distilled water so that total solution is 100 ml.

Phosphate buffer : 0.30 mol / L

DTNB : 40 mg 5,5'-Dithiobis (2-nitrobenzoic acid) is solved inside 1% sodium sitrate (Na_2HPO_4)solution.

GSH standard : 10 mg/dL – 50 mg/dL

The cuvets are prepared as given below:

	Blind	**Standard**	**Assay**
GSH calibrator	-	2 ml	-
Erythrocyte	-	-	2 ml
Precipitating reagent	1.2 ml	-	-
After incubating at room temperature for 5 minutes, the solution is centrifuged at 3000 cycles/min for 10 minutes. Upper phase is extracted and the following materials are added on it:			
Phosphate buffer	8 ml	8 ml	8 ml
DTNB	1 ml	1 ml	1 ml
Distilled water	0.8 ml	-	-

The color reading is performed at 412 nm against the blind solution in 4 minutes.

The calculation is accomplished by using glutathione standard curve.

5.3 SOD Determination

The method of determination of SOD activity is based on the reduction of nitroblue tetrazolium by superoxide anions that are formed by xanthine/xanthine-oxidase system and then inhibition of superoxide anions by SOD. Reaction mixture used to determine the SOD activity is prepared using the following molecules at the specified concentrations inside a 200 ml flask.

Reaction Mixture

Molecule	**Concentration**
Xanthine	0.3 mmol / L
EDTA	0.6 mmol / L
Nitroblue tetrazolium	150 μmol / L
Na_2CO_3	400 millimol / L
Bovin serum albumin	1 g / L

Reaction mixture is set to a pH level of 10.2.

As a first step in SOD determination, supernatant solution is prepared using the following molecules at the specified amounts:

Supernatant solution

Molecule	**Concentration**
Chloroform letanal	400 μmol
Erythrocyte	50 μmol
Distilled water	450 μmol

This solution is centrifuged at 15000 cycles/min for 10 minutes.

At the second step, the determination is performed according to the protocol given below:

	Blind (ml)	Test (ml)
Reaction mixture	1	1
Distilled water	0.02	-
Supernatant solution	-	0.02
Xanthine oxidase (0.167 U/ml)	0.05	0.05
incubated at 25 ^{o}C for 20 minutes. Then adding		
$CuCl_2$ (8 mmol/L)	0.05	0.05
the reaction is stopped.		

The formazan formation of both the blind and the specimen is measured using spectrophotometer which is set to 560 nm wavelength.

$$\% \text{ inhibition} = 100 \text{ x } \frac{A_{blind} - A_{test}}{A_{blind}} \qquad (5.2)$$

where A is the absorbance value read by the spectrophotometer.

According to Sun modifying method, the 50 % inhibition with respect to the blind inside the reaction tube corresponds to 1 unit of SOD activity.

The units of SOD activity is determined by simple linear ratio. But it has to be further determined with respect to the hemoglobin concentration inside the solution, so the resultant SOD activity is formulated in terms of Units / gram hemoglobin (or U / g Hb).

The hemoglobin concentration, on the other hand, is determined using the Drabkin's reagent, which is given below:

Drabkin's reagent

Molecule	**Concentration**
$K_3Fe(CN)_6$	0.198 g
KCN	0.052 g
$NaHCO_3$	1 g
Distilled water	Added to complete to 1 L.

The procedure is as follows:

1. Pipet 3.0 mL of Drabkin's reagent into a disposable cuvet.
2. Add 0.2 mL of 1:20 hemolysate. Mix.
3. Place in the dark and allow to incubate for 10 min at room temperature.
4. Read absorbance at 540 nm against a blank of Drabkin's solution.
5. Determine the hemolysate hemoglobin concentration from a calibration curve [46, 47].

6. RESULTS

6.1 Biochemical Analysis Results

Levels of all the three biochemical parameters of interest have been changed significantly under EM radiation effect. MDA level was increased significantly ($p<0.0001$) for the experiment group (10.20 ± 0.78 mM/L) when compared to the sham-exposed group (6.77 ± 0.60 mM/L). SOD activity was also increased for the experiment group (2.53 ± 0.87 Units / mg Hb), although less significantly ($p=0.019$), when compared to the sham-exposed group (1.79 ± 0.72 Units / mg Hb). GSH concentration, on the other hand, decreased significantly ($p<0.0001$) for the experiment group (7.84 ± 1.15 mg / g Hb) when compared to the sham exposed group (19.19 ± 1.64 mg / g Hb) [49, 50]. Details of the results are given in following subsections.

6.1.1 Malondialdehyde Analysis Results

Results of malondiladehyde analysis are shown in Table 6.1 and Figure 6.1.

Table 6.1 Malondialdehyde levels measured in each rat after exposure to electromagnetic radiation and after sham exposure.

Group I (Experiment)		**Group II (Sham Exposure)**	
Rat ID	**MDA Level (mMol / L)**	**Rat ID**	**MDA Level (mMol / L)**
101	9.11	300	6.54
102	10.95	301	6.65
103	11.06	302	6.98
110	9.22	303	7.82
120	10.17	310	6.14
130	9.72	320	6.03
133	9.83	321	6.26
140	10.73	322	7.15
143	11.06	330	7.37
Avg. ± Std.Dev.	***10.20 ± 0.78***	***Avg. ± Std.Dev.***	***6.77 ± 0.60***

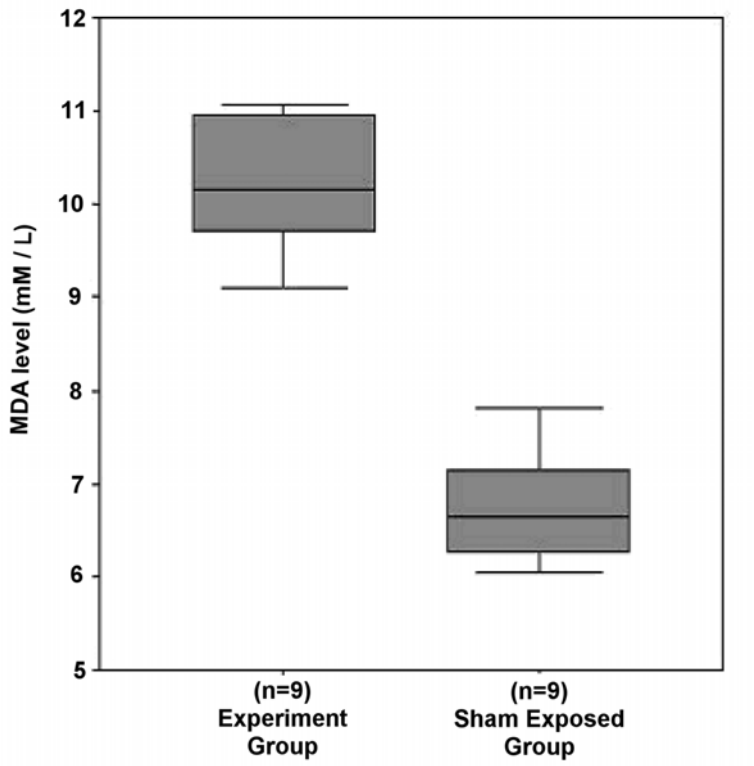

Figure 6.1 Effects of 945 MHz electromagnetic radiation on lipid peroxidation levels in rat blood samples (mean ± standard deviation). $p<0.0001$ vs. sham according to Mann-Whitney U test.

6.1.2 Glutathione Analysis Results

Glutathione analysis results are shown in Table 6.2 and Figure 6.2.

Table 6.2 Glutathione levels measured in each rat after exposure to electromagnetic radiation and after sham exposure.

Group I (Experiment)		**Group II (Sham Exposure)**	
Rat ID	**GSH Level (mg / g Hb)**	**Rat ID**	**GSH Level (mg / g Hb)**
101	9.81	300	17.91
102	6.71	301	20.32
103	7.23	302	20.49
110	8.26	303	20.66
120	8.61	310	18.25
130	9.13	320	18.08
133	7.06	321	19.80
140	7.23	322	16.18
143	6.54	330	21.00
Avg. ± Std.Dev.	***7.84 ± 1.15***	***Avg. ± Std.Dev.***	***19.19 ± 1.64***

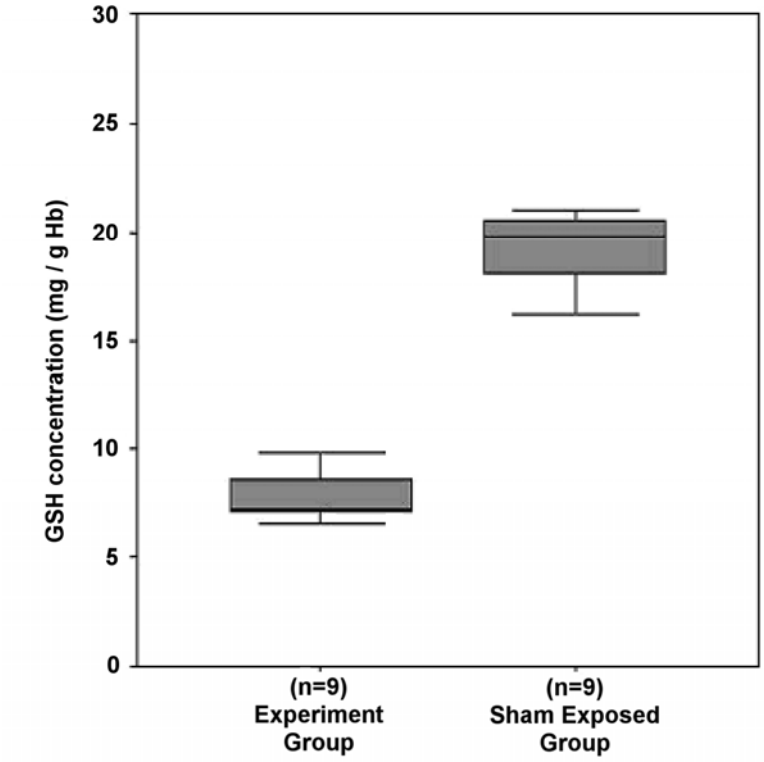

Figure 6.2 Effects of 945 MHz electromagnetic radiation on glutathione concentration in rat blood samples (mean ± standard deviation). $p<0.0001$ vs. sham according to Mann-Whitney U test.

6.1.3 Superoxide Dismutase Analysis Results

Superoxide Dismutase analysis results are shown in Table 6.3 and Figure 6.3.

Table 6.3 Superoxide dismutase levels measured in each rat after exposure to electromagnetic radiation and after sham exposure.

Group I (Experiment)		**Group II (Sham Exposure)**	
Rat ID	**SOD Level (Units / mg Hb)**	**Rat ID**	**SOD Level (Units / mg Hb)**
101	2.63	300	1.44
102	2.23	301	1.71
103	1.92	302	1.53
110	4.65	303	1.38
120	1.73	310	0.99
130	2.01	320	1.47
133	2.14	321	2.03
140	2.77	322	3.47
143	2.67	330	2.13
Avg. ± Std.Dev.	***2.53 ± 0.87***	***Avg. ± Std.Dev.***	***1.79 ± 0.72***

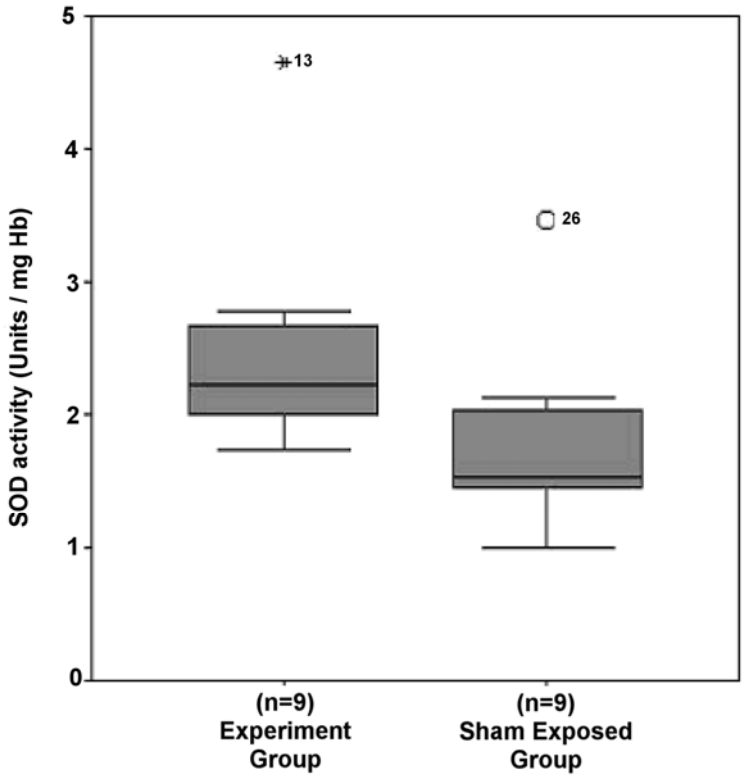

Figure 6.3 Effects of 945 MHz electromagnetic radiation on superoxide dismutase activity in rat blood samples (mean ± standard deviation). p=0.019<0.050 vs. sham according to Mann-Whitney U test.

6.2 Other Biological Parameters of Interest

6.2.1 Leukocyte Analysis

Number of lymphocytes found on blood samples collected from rats before and after electromagnetic exposure and sham exposure are given in Table 6.4.

Table 6.4 Change in lymphocyte count for the experiment and sham exposure groups.

Group I (Experiment)			Group II (Sham Exposure)		
Rat ID	Lymphocytes Before Exposure	Difference After Exposure	**Rat ID**	Lymphocytes Before Exposure	Difference After Exposure
101	84	-22	300	58	-8
102	66	18	301	62	14
103	65	9	302	79	-9
110	77	6	303	77	7
120	72	-4	310	73	-5
130	(*)	(*)	320	83	-43
133	82	-27	321	80	-17
140	62	4	322	65	-22
143	70	-12	330	73	8
Average	72	-3	Average	72.22	-8.3

(*) No sample was taken for this rat.

Number of polymorphonuclear leukocytes (PNL) found on blood samples collected from rats before and after electromagnetic exposure and sham exposure are given in Table 6.5.

Table 6.5 Change in PNL count for the experiment and sham exposure groups.

Group I (Experiment)			Group II (Sham Exposure)		
Rat ID	PNL Before Exposure	Difference After Exposure	**Rat ID**	PNL Before Exposure	Difference After Exposure
101	15	22	300	40	7
102	19	-6	301	35	-14
103	32	-10	302	19	9
110	22	-8	303	22	-7
120	22	6	310	25	4
130	(*)	(*)	320	17	41
133	16	28	321	19	16
140	35	-3	322	32	21
143	24	16	330	25	-8
Average	23	5	Average	26	8

(*) No sample was taken for this rat.

6.2.2 Urine Analysis

Vanil mandelic acid (VMA) levels in rats at proceeding days of the experiment are given in Table 6.6.

Table 6.6 VMA analysis results for the experiment and sham exposure groups.

Days	Group I (Experiment)		Group II (Sham Exposure)	
	Sample Volume (ml)	VMA Level (mg / L)	Sample Volume (ml)	VMA Level (mg / L)
3rd day	16.00	4.80	55.20	12.25
5th day	25.00	6.35	67.75	12.30
7th day	19.00	10.25	44.20	44.15
9th day	12.00	9.80	57.30	40.70

7. DISCUSSION AND CONCLUSION

A two-phase experiment was designed in order to investigate the effects of EM fields at GSM BTS transmitter frequencies. In the first phase, EM field at 945 MHz of 3.67 W/m^2 power density, which is calculated to produce a SAR value of 11.3 mW/kg, was applied on a group of 9 rats inside a GTEM Cell. In the second phase, the same number of rats was sham exposed under the same conditions. The duration was 7 hours/day for a period of 8 days, in each phase.

A decrease in lymphocyte levels in both groups is observed. This decrease can be attributed to the stress the animals are exposed to. Stress can be indicated as psychological and biological response of the animals to the threatening circumstances. The unusual GTEM Cell environment could be the source of anxiety. According to previous studies [51, 52, 53], the total number of lymphocytes in blood diminishes as a result of controlled stress exposed on rats and some other biological organisms. An increased polymorphonuclear leukocyte (PNL) level with a decrease in lymphocyte count is reported, which is also in agreement with our findings.

Analyses of the urine samples, gathered every two days, from the two cages indicate an increasing level of vanil mandelic acid (VMA) concentration for both phases of the experiment. VMA increase is more pronounced for the sham exposed group. Increase in VMA is attributed to; acute anxiety, very rarely ganglioblastoma or ganglioneuroma, rarely neuroblastoma or pheochromocytoma, and severe stress [54]. Since none of the pathologies mentioned here existed in the subject animals we can conclude the increased level of VMA concentrations is also due to the increased level of anxiety and stress of the animals caused by the experiments.

Biochemical analysis of blood samples indicate that the GSM BTS EM radiation exposed rats have higher concentration levels of MDA (malondialdehyde) and lower GSH (glutathione) concentrations when compared to the sham exposed group. This outcome is in agreement with the results of some previous studies. Daşdağ et al. [9] studied the effects of mobile phone EM radiation on rat brain tissues, where rats are exposed to EM fields for

20 min/day for 30 days (SAR=0.52 W/kg). The MDA levels in rat brain tissues increased significantly after exposure. In another study by Özgüner et al. [11], renal impairment in rats was investigated under mobile phone radiation (SAR=0.016 W/kg). Rats were exposed 30 min/days for 90 days and the result was increase of renal tissue MDA, NO (nitric oxide) and urinary NAG (N-acetyl-β-D-glucosaminidase) levels and significant decrease of tissue SOD, CAT (catalase) and GSH-Px (glutathione peroxidase) levels. Ilhan et al. [10] studied mobile phone induced oxidative stress in rat brain. Rats were exposed to mobile phone emissions (SAR=0.25 W/kg) for 1 hour/day for 7 days. MDA and NO levels were increased whereas GSH-Px and SOD activities were decreased significantly in rat brain tissue. Additionally, XO (xanthine oxidase) and ADA (adenosine deaminase) levels were also increased. Moreover, Moustapha et al. [55] have studied acute mobile phone exposure effects on human volunteers and found out that MDA level in plasma was increased and GSH-Px and SOD activities were decreased in human erythrocytes after 1h, 2h and 4h of exposure. No significant change was observed for CAT activity in this study.

However, some other studies in literature have concluded in no relation between EM field exposure and free radical activity. Irmak et al. [56] have shown that EM radiation from mobile phones applied 30 min/days for 7 days on rabbits had no significant effect on rabbit brain, suggesting that oxygen free radicals were not generated. But, they have observed a significant increase in serum SOD activity in the exposed group. In addition, Zmyslony et al. [8] have exposed rat lymphocytes in vitro to 930 MHz continuous wave (CW) radiation inside a GTEM Cell (SAR=1.5 W/kg). Five min and 15 min acute exposure resulted in no change in reactive oxygen species production in living cells. However, change was observed when lymphocytes were treated with $FeCl_2$ as a stimulating agent.

In the scope of REFLEX project, a series of experiments was performed on human promyelocytic HL-60 cells to examine whether RF-EMF (1800 MHz at SAR 1.3 W/kg, 24h exposure) is capable to induce indirect genotoxic effects by affecting the generation and elimination of reactive oxygen species (ROS). For monitoring these ROS-formation and elimination steps, different assays, measuring nitric oxide, oxyDNA, oxidative DNA-damage via Dihydrorhodamine 123 (DHR123), lipid peroxidation, glutathione peroxidase activity, superoxide dismutase activity, have been established and were applied following RF-field exposure of HL-60 cells at that exposure condition with the most significant

effect on DNA integrity (1800 MHz, continuous wave, 1.3 W/kg, 24h). By applying sequential approaches for the detection of reactive oxygen species (ROS) in HL-60 cells, an increase in the intracellular generation of free radicals accompanying RF-EMF exposure could be clearly demonstrated by flow cytometric detection of the oxidized nucleotide 8-oxoguanosine (oxy-DNA assay) and the fluorescent Rhodamine 123 (DHR 123 assay), respectively. To screen the possible effect of RF-EMF on endogenous antioxidant enzyme activity, the activities of superoxide dismutase (SOD) and glutathione peroxidase (GSH-Px) were determined in the HL-60 cells that were exposed to RF-fields (1800 MHz), continuous wave, SAR 1.3 W/kg for 24h. However, RF-EMF did not affect antioxidant enzyme activities of HL-60 cells (SOD and GSH-Px activity). On the other hand, it was found that the generation of genotoxic effects through RF-EMF was inhibited by ascorbic acid, which is a well-known antioxidant [30].

There are experimental evidences that oxidative stress and consequent free radical production are important causative factors in the pathology of several degenerative disorders. In a Parkinson's disease model SOD, CAT and GSH-Px activities were increased in striatum and ventral midbrain of mice [57]. In another Parkinson's disease model Thiffault et al. [58] showed an increase in SOD activity with no increase in GSH-Px activity in mice brain. Neuronal GSH deficiency and age dependent neurodegeneration were found to be related with the downregulation of excitatory amino acid transporters in mice [59].

According to our results, MDA level and SOD activity were increased, whereas GSH concentration was decreased in EM radiation exposed rats when compared to sham-exposed group. We think that decreased GSH concentration may be due to the higher consumption of GSH for scavenging the higher production of free radicals. The lower GSH concentration may have some relation to the increased SOD activity. Note that the endogenous GSH has a protective function in scavenging radicals and in molecular repair. However, such scavenging can set up a superoxide-dependent chain production of H_2O_2 and oxidized glutathione, which would oxidatively stress the cell. Therefore, the increased SOD activity may be a response to suppress the higher chain oxidation of GSH, or a response to balance the decreased GSH concentration.

Thus, the upregulated SOD activity converts $O_2\cdot^-$ to H_2O_2 and downregulated GSH concentration leads to the insufficient detoxification and accumulation of H_2O_2 in the system. H_2O_2 is known to be converted to hydroxyl radical in the presence of iron rapidly,

which is the most damaging form of ROS. Note that the balance between GSH-Px and SOD appears to be important for the cellular resistance to oxidative stress [60].

In conclusion, our results indicate that exposure to EM fields at BTS frequencies may modulate the oxidative stress of free radicals by enhancing lipid peroxidation and reducing the concentration of GSH. It is highly probable that detoxification of lipid peroxyl radicals can not be accomplished in our system. We note that reactive oxygen species may have a probable role on adverse effects of EM fields at mobile telecommunication frequencies, as also emphasized in the conclusion of the REFLEX project final report [30]. The outcome of this study needs confirmation by repetitive laboratory studies, including higher dose and longer duration exposure, and theoretical mechanisms underlying this effect should also be addressed in future.

APPENDIX A

APPENDIX A. RF FIELD MEASUREMENT AND THEORETICAL CALCULATION FOR CELLULAR BASE STATION ANTENNAS

A.1 Introduction

Characterization of the RF source is very important since biological effects are mostly dependent on the field strength level, frequency and signal characteristics. Many analytical and numerical techniques have been used to obtain the radiation characteristics of these antennas so far. The analytical solution given in the next section is taken from a poster paper presented at 4th International Symposium on Electromagnetic Compatibility and Electromagnetic Ecology, 19 – 22 July 2001, St.Petersburg, Russia [61].

A.2 Analytical Solution

Usually the radiation pattern of a single element is relatively wide, and each element provides low values of directivity (gain). In many applications, it is necessary to design antennas with very directive characteristics (very high gains) to meet the demands of long distance communication. This can only be accomplished by increasing the electrical size of the antenna.

One way to enlarge the dimensions of the antenna, without necessarily increasing the size of the individual elements, is to form an assembly of radiating elements in an electrical and geometrical configuration. This new antenna consist of multi elements and is called as “an array”. The total field of the array is determined by the vector addition of the fields radiated by the individual elements.

A.2.1 Four - Element Array

Base anttennas are formed by using half-wavelength dipole as a collinear array. The total radiation of this array-antenna is obtained analytically. The antenna under investigation is an array of four vertical dipoles positioned along the z-axis,behind a metallic reflector, as shown in Figure A.1.

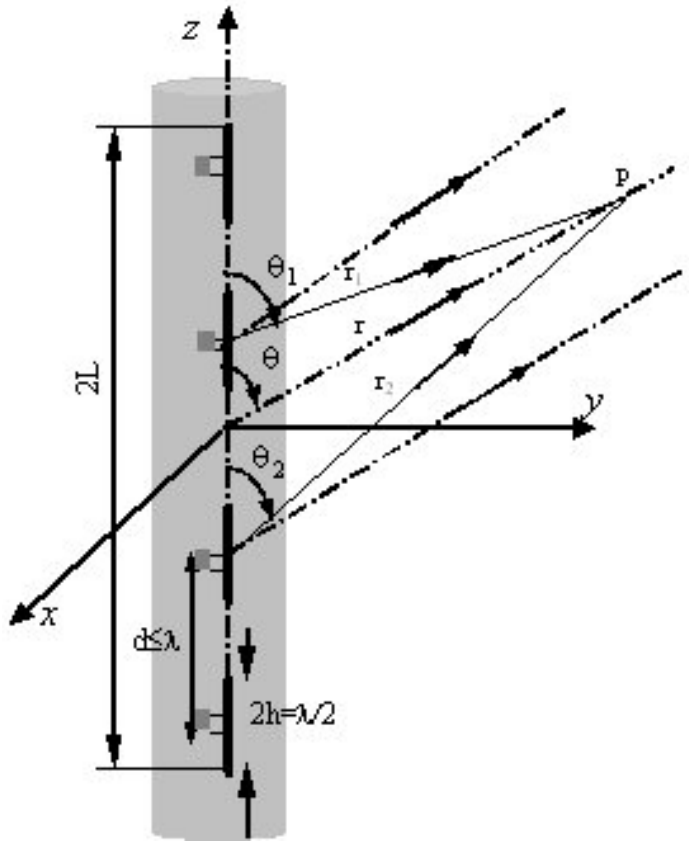

Figure A.1. Schematic view of the studied dipole array antennas

The field at an observation point P can be described as the sum of fields radiated by four dipoles in the presence of the reflector.

$$\vec{E}_t = \vec{E}_1 + \vec{E}_2 + \vec{E}_3 + \vec{E}_4 \qquad \text{(A.1)}$$

$$E_t = \mathrm{j}\eta \frac{kI_0 l}{4\pi r} f(\theta) e^{-j\beta r} \left[1 + \zeta_1 e^{j(\alpha_1 + \beta \vec{a}_r \vec{r}_1)} \ldots\ldots \right.$$
$$\left. \ldots\ldots \underbrace{+ \zeta_1 e^{j(\alpha_i + \beta \vec{a}_i \vec{r}_1)} \ldots + \zeta_{n-1} e^{j(\alpha_{n-1} + \beta \vec{a}_i \vec{r}_{n-1})}}_{\text{Array Factor (AF)}} \right] \quad \text{(A.2a)}$$

$$\frac{I_i}{I_0} = \zeta_i e^{j\alpha_i} \quad \text{(A.2b)}$$

$$f(\theta) = \frac{\cos(\frac{\pi}{2}\cos\theta)}{\sin\theta} \quad \text{(A.2c)}$$

where;

η is the free-space wave impedance

k is wave number

l is dipole length ($l = \lambda / 2$ for half-wave dipole)

$f(\theta)$ is radiation pattern factor of unit antenna (half-wave dipole)

r is distance between antenna and point P

I_0 is electric current on unit antenna

ζ_i is electric current on i-th antenna

$\vec{a}_r$ is unit vector on r-direction in spherical coordinates

$\vec{r}_i$ is position vector i-th antenna.

Total field has been illustrated so that the far-zone field of uniform four-element array of identical elements is equal to the product of the field of single element, at a selected reference point (usually the origin), and the array factor of that array. That is

$$\mathrm{E} = [\mathrm{E}_{(\text{single element})}] \text{ x } [\text{Array factor (AF)}] \quad \text{(A.3)}$$

$$AF = \sum_{n=1}^{N} e^{j(n-1)\psi_z} \quad \text{(A.4a)}$$

$$\psi_z = \alpha_z + \beta d_z \cos(\theta) \quad \text{(A.4b)}$$

After some mathematical manipulations Equation A.4a reduces to

$$(AF)_n = \frac{1}{N}\left[\frac{\sin(\frac{N}{2}\psi)}{\sin(\frac{\psi}{2})}\right] \tag{A.4c}$$

The total field of four half-wave dipole z-axis have been obtained analitically,

$$E_{tz} = j\eta\frac{I_0}{2\pi r} f(\theta,\phi)\left[\frac{\sin(\frac{N_z}{2}\psi_z)}{N_z \sin(\frac{\psi_z}{2})}\right] e^{-j\beta r} \tag{A.4d}$$

The contribution of metallic reflector can be added to Equation A.4d by using image theory.

$$E_{tzy} = E_{tz}\left[\frac{\sin(\frac{N_y}{2}\psi_y)}{N_y \sin(\frac{\psi_y}{2})}\right] \tag{A.5a}$$

$$\psi_y = \alpha_y + \beta d_y \sin(\theta)\cos(\phi) \tag{A.5b}$$

To find the nulls of the array on the z-axis, Equation A.4d are set equal to zero. That is,

$$\theta_{nz} = \cos^{-1}\left[\frac{\lambda}{2\pi d_z}(-\alpha_z \pm \frac{2n_z}{N_z}\pi)\right] \quad \mathrm{n}_z = 1,2,3... \qquad \mathrm{n} \neq N_z, 2N_z, 3N_z... \tag{A.6}$$

The maximum values of Equation A.4d occur when

$$\theta_{mz} = \cos^{-1}\left[\frac{\lambda}{2\pi d_z}(-\alpha_z \pm 2m\pi)\right] \quad \mathrm{m}_z = 0,1,2,3...$$

$$\theta_m = \cos^{-1}\left[\frac{\lambda\alpha_z}{2\pi d_z})\right] \quad \mathrm{m} = 0 \tag{A.7}$$

The 3-dB point for the array factor Equation A.4d occurs when

$$\theta_{hz} = \cos^{-1}\left[\frac{\lambda}{2\pi d_z}(-\alpha_z \pm \frac{2.782}{N_y}\pi)\right] \quad \text{n} = 1,2,3... \qquad \text{(A.8)}$$
$$\text{n} \neq N_z, 2N_z, 3N_z.$$

By the same way to find the nulls, the maximum values and the 3-dB point of the array on the y-axis occur when,

$$\theta_{ny} = \cos^{-1}\left[\frac{\lambda}{2\pi d_y}(-\alpha_y \pm \frac{2n}{N_y}\pi)\right] \quad \text{n}_\text{y} = 1,2,3...$$
$$\text{n} \neq N_y, 2N_y, 3N_y...$$
$$\theta_{my} = \cos^{-1}\left[\frac{\lambda}{2\pi d_y}(-\alpha_y \pm 2m\pi)\right] \quad \text{m}_\text{y} = 0,1,2,3...$$
$$\theta_{my} = \cos^{-1}\left[\frac{\lambda\pi\alpha_y}{2\pi d_y})\right] \quad \text{m} = 0 \qquad \text{(A.9)}$$
$$\theta_{yh} = \cos^{-1}\left[\frac{\lambda}{2\pi d_y}(-\alpha_y \pm \frac{2.782}{N_y}\pi)\right] \quad \text{n}_\text{y} = 1,2,3...$$
$$\text{n} \neq N_y, 2N_y\ 3N_y.$$

In this problem,

N_z=4,

N_y=2,

$\lambda = 0.33\text{m}$

$d_z = \frac{\lambda}{2}$

$d_y = \frac{\lambda}{4}$

$\psi_z = \pi\cos(\theta)$

$\psi_y = \pi + \frac{\pi}{4}\sin(\theta)\cos(\phi)$,

The radiation patterns obtained rom this calculation are given in Figure A.2 and Figure A.3.

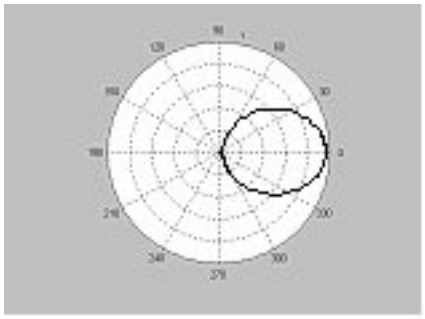

Figure A.2 The radiation pattern of the array on the z-axis in the horizontal plane for 900 MHz.

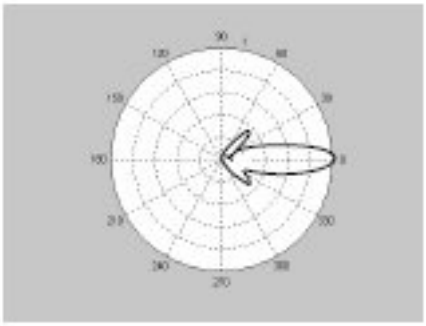

Figure A.3 The radiation pattern of the array on the z-axis in the vertical plane for 900 MHz.

APPENDIX B

APPENDIX B. SPECIFIC ABSORPTION RATE CALCULATION

B.1 Theory

In biological experiments the field strengths induced in the tissues should be defined as well as possible. Profound knowledge of the absorption mechanism is needed for evaluation of an optimal exposure system. However, any setup should be complemented by numerical or experimental dosimetry, since a thorough dosimetry is a prerequisite for a good biological study. Field strength variations in the target tissues (e.g. due to different anatomies and movement) must be determined with the greatest precision. The exposure of the remaining tissues should be reliably assessed as well. In most cases this can be best achieved using numerical techniques. Since the possible errors in numerical simulations are numerous, solutions must be validated. The correctness of the simplifications must also be validated. This is best achieved by measurements in critical areas or by applying a second independent numerical technique [62].

The most obvious approach towards dosimetric analysis is to experimentally determine the specific absorption rate (SAR) distribution in phantoms simulating animal and human bodies as well as real cadavers. One possibility to determine the local or whole-body SAR is by temperature measurements. The SAR is proportional to the temperature increase only when the effects of heat diffiusion can be neglected. Because of thermodynamic processes, this is only the case at the moment the exposure begins ($t \rightarrow +0$) and when thermal equilibrium existed at the site of measurement prior to the exposure

$$SAR = c\,(\partial T / \partial t) \qquad \text{when } (t \rightarrow 0) \tag{B.1}$$

where c is the specific heat of the tissue at the site of measurement. Since the heat transfer mechanisms that lead to thermal equilibrium are relatively slow, SAR can be determined by evaluating c ($\Delta T/\Delta t$) if the effects of thermal conduction, convection and radiation are

negligible in the time interval Δt. In fluids with relatively low viscosity, convection is the dominant heat transfer mechanism. Since convection is a non-linear process, assessment of the SAR by taking measurements over a longer period of time (> 30 - 60 s) and accounting for heat exchange processes is very intricate and should be avoided.

Another way of determining the SAR distribution inside tissue-simulating materials is by measuring the electric field (E_i) inside the exposed tissue:

$$SAR = \sigma \, |E_i|^2 / \rho \qquad (B.2)$$

where σ is the conductivity, ρ the density of the tissue at the site of the measurement, $|E_i|$ is the Hermitian magnitude of the local electric field vector.

Both approaches have some common requirements. Any field disturbance caused by the probe must be avoided. A further requirement, which is often but not necessarily concomitant with the previous, is that any signal picked up by any part of the probe other than the sensor itself should be sufficiently suppressed. For tests of compliance with safety limits a sensitivity at least a magnitude better than the safety limits is required, since unmodified equipment is preferably to be tested. A sensitivity of at least 0.1 W/kg would certainly satisfy these requirements, which approximately corresponds to 0.03 mK/s or 10 V/m for current liquids or gels simulating tissues rich in water.

The spatial resolution should be better than the smallest spatial dimension of any local field maximum or minima, in order to enable accurate assessment of the SAR distribution. Compliance tests and most dosimetric assessments require the determination of the SAR distribution in the tissue volume of interest. In larger volumes with greatly non-uniform distributions, measurements at several hundred points might be necessary. Since the location of the sensor must be precisely known, stereotactic or robot positioning is a costly but often necessary solution.

B.2 Temperature Measurement Methods

An important advantage of the temperature measurement method is that temperature is a scalar, which makes it easier to produce probes of very small size and short time constants. One major difficulty is to achieve high SAR sensitivity, i.e., << 1 W/kg. Another important drawback is that the time derivative can be determined only by temperature measurements at two discrete times, whereby the thermodynamic state prior to exposure must be known and preferably be in equilibrium. Since the exposure alters thermal equilibrium, some means and time must be provided to re-establish equilibrium after each measurement cycle.

B.2.1 Implantable Electrical Temperature Probes

A temperature probe based on a high-resistance thermistor connected to high-resistance leads was first described by Bowman. By using the four-lead configuration, a high impedance current source and voltage amplifier, the temperature can be measured accurately, despite the instability and temperature dependence of the leads. Such probes are commercially available and have been successfully used in dosimetry in the last two decades. Excellent sensitivity (see Table B.1) has recently been achieved by using specialized electrometer grade amplifiers and sophisticated software for filtering and data evaluation. One disadvantage is that the leads of these probes are not totally unaffected by electromagnetic fields.

B.2.2 Implantable Optical Temperature Probes

In the eighties, temperature sensors utilizing optical temperature effects were developed and commercialized for applications such as temperature control in high voltage transformers, industrial microwave heating, hyperthermia, dosimetry, etc. One of the effects employed for temperature measurements is the rate of fluorescent decay from a phosphorescent layer on the tip of an optical fibre. An exponentially-decaying material with a long half life is preferably used (e.g., magnesium fluorofermanate activated with tetravalent manganese excitable by Xenon flash light. Currently commercially available

devices typically do not have a noise level of better than ± 0.1 ^{o}C (averaging time 1 s). Multichannel devices with a wide operational range from -200 ^{o}C to 450 ^{o}C are now available.

Another effect that has been utilized for optical probes is the interferometric microshift of a cavity resonator, which is filled with a material of very high temperature - dependent refractive index. The short-term drifts and noise are about 10 mK/s for practical applications. This can be reduced by improved data processing. In small animal cadaver a sensitivity of about 2-3 mK/s was achieved due to the larger thermal constant in the tissue compared to liquids.

Table B.1 Comparison of Commercially Available Temperature Measurement Systems.

Physical Principle	**Fluorescent Decay**	**Cavity Resonator**	**Thermistor**
Noise level / short term drifts (sampling time)	± 0.1 ^{o} C (1 s)	± 0.1 ^{o} C	± 0.005 ^{o} C (10 s)
Sensitivity (10 s of exposure)	± 15 mK/s	± 10 mK/s	± 0.15 mK/s
Sensitivity to RF exposure (835 MHz)			
- resistive lines parallel to E-field	< noise	< noise	< 0.5 mK/s *
- resistive lines normal to E-field	< noise	< noise	< 0.1 mK/s *

(*) Measured by exposing the first 6 cm of the line from the tip to an incident field of 950 V/m.

B.2.3 Radiation Thermometry

Radiation thermometry was one of the first methods utilized for SAR measurements. The technology for infrared imaging has been continuously improved since then, and sophisticated devices for various applications (e.g., medical diagnosis, infrared sensing, etc.) are today available. However, the sensitivity of >10 W/kg achievable in practice is not sufficient. In addition this technique is limited to certain cross sections.

B.2.4 Calorimeters

A variety of calorimeters has been used to measure the total energy delivered to a whole-animal cadaver. Although this method is accurate in the determination of whole-body averaged SAR, it cannot provide information about the SAR distribution within the body.

B.3 Electrical Field Measurement Methods

E-field probes have been utilized since the early 70s for experimental measurement of RF fields inside tissue simulating liquids. The first prototype of a miniature isotropic diode loaded E-field probe for dosimetric assessments was presented by Bassen.

The use of fiber optical E-field sensors for dosimetric assessments was suggested as far back as 1978, although it has taken present day technology for commercial application.

Since the field polarization is unknown in the close near fields of radiators, only probes with an isotropic response in the tissue simulating material should be used. This is accomplished by measuring the field components with three orthogonal sensors. Because of the short wave length in the tissue and since the induced field may have relatively large spatial gradients, the probe size should be as small as possible. Furthermore, the interaction of the probe with the field should be negligible.

These requirements are difficult to satisfy, because the usually fragile sensors must be mounted on a supporting core and covered with an outer shell to strengthen the probe tip and to protect the single probes from contact with the tissue simulating material. However, any dielectric material around electric probes has an effect on the local signal strength, depending on the surrounding material. A good orthogonal response in a particular material might be greatly impaired in another media. In addition, the sensitivity of these probes in lossy media depends on the frequency and to a lesser extent also on the relative permittivity of the media.

B.3.1 Diode Loaded Dipole Sensors

Isotropic diode loaded dipole sensors consist of three small orthogonal arranged dipoles which are directly loaded with Schottky diodes. Direct conversion of the high frequency voltage across the gap into a DC voltage and highly resistive lines (RF transparent) are used to transmit the DC signal to the data acquisition unit. The resistive lines have been realized either by carbon-impregnated Teflon strips, thin-film or thick-film technology on a ceramic or quartz substrate. Different probes are currently commercially available.

B.3.2 Fiber Optical E-Field Sensors

Several groups world-wide are currently developing fiber optical E-field sensors for various applications using the Pockels effect. The Pockels effect describes the change in the optical dielectric permittivity of noncentrosymmetric crystals, which is linear with the electric field. This effect is used in many integrated optics devices to alter the real or imaginary index of refraction (i.e., tuning of a fiber optical switches, modulators, etc.) but can also be used to realize E-field sensors. The promising advantages of this approach are that these sensors are non-metallic, extremely broad band (practically from DC to several GHz) and enable measurements in the time domain, i.e., provide frequency and phase information.

Such sensors are already commonly used in high-voltage applications. A small wideband sensor on a $LiNbO_3$ substrate is realized, whereby the E-field induced in the crystal is enhanced by attached metallic dipole arms. Another approach has been recently presented, which is based on a CdTe (Cadmium Telluride) crystal and has relatively low permittivity. The one-dimensional probe has no attached metallic dipole arms but a sensing crystal of about 10 mm length. None of these probes is currently commercially available.

B.3.3 Calibration of E-Field Probes

Reliable and accurate standard procedures must be available to calibrate E-field probes in the different tissue simulating liquids and to assess the uncertainties in assessing the spatial peak SAR values. Keeping uncertainties small is crucial for compliance tests, since all uncertainties must be added to the measured values

In a recent study the calibration issue has been analyzed in detail and an experimental procedure has been developed which allows an absolute calibration of the probes for dosimetric assessments with an uncertainty of less than ± 10%.

B.4 Discussion

The required sensitivity for compliance tests of 10 V/m can easily be met by electrical field measurement methods. The loss of phase and frequency information is no disadvantage for the dosimetric analysis of near field exposure, since the signal characteristic is known "a priori". Although the smallest achievable dimensions are still considerably larger than those of temperature probes, they are sufficiently small for measurements inside human phantoms and for the frequencies used by mobile communications. A disadvantage is that special calibration data are required for each material. However, this is not a problem for routine measurements such as device certifications, which are always conducted with a limited number of different tissues and narrow frequency bands.

Fiber optic sensors are currently not a real alternative to the diode loaded sensors, because of the lack of sensitivity and particularly because of the significantly larger dimensions of the sensors and more expensive technology [63].

REFERENCES

1. ICNIRP, "Guidelines for limiting exposure to time-varying electric, magnetic and electromagnetic fields (up to 300 GHz)", *Health Physics*, pp.494-522, Vol.74, 1998.

2. CENELEC, "EN 50360 - Product standard to demonstrate the compliance of mobile phones with the basic restrictions related to human exposure to electromagnetic fields (300 MHz - 3 GHz)", European Standards Organization. Directive 199/5/EC on Radio Equipment and Telecommunications Terminal Equipment and the mutual recognition of their conformity, 2001.

3. Telekomünikasyon Kurumu, 10 kHz - 60 GHz Frekans Bandinda Çalisan Sabit Telekomünikasyon Cihazlarindan Kaynaklanan Elektromanyetik Alan Siddeti Limit Degerlerinin Belirlenmesi, Ölçüm Yöntemleri ve Denetlenmesi Hakkinda Yönetmelik, Resmi Gazete, No.24460, 12/07/2001.

4. IEGMP, "Mobile Phones and Health", Report of Independent Expert Group on Mobile Phones. National Radiation Protection Board Report. Oxon, UK, 2000. Available from: http://www.iegmp.org.uk/report/text.htm.

5. Sienkiewicz, Z.J. and Kowalczyk C.I., "A Summary of Recent Reports on Mobile Phones and Health (2000–2004)", National Radiation Protection Board Publication. W65. UK, 2005. Available from: http://www.hpa.org.uk/radiation/publications/w_series_reports/2005/nrpb_w65.htm.

6. Brocklehurst, B. and McLauchlan, K.A., "Free radical mechanism for the effects of environmental electromagnetic fields on biological systems", *Int J Radiat Bio*, pp.3-24, Vol.69, 1996.

7. Lacy-Hubert, A., Metcalfe, J.C. and Hesketh, R., "Biological responses to electromagnetic fields", *FASEB Journal*, pp. 395-420, Vol.12, 1998.

8. Zmyslony, M., Politanski, P., Rajkowska, E., Szymczak, W. and Jajte J., "Acute exposure to 930 MHz CW electromagnetic radiation in vitro affects reactive oxygen species level in rat lymphocytes treated by iron ions", *Bioelectromagnetics*, Vol.25, pp. 324-328, 2004.

9. Dasdag, S., Akdag, M.Z., Aksen, F., Bashan, M. and Büyükbayram, H., "Does 900 MHz GSM Mobile Phone Exposure Affect Rat Brain?", *Electromagnetic Biology and Medicine*, pp.201-214, Vol.23, 2004.

10. Ilhan, A., Gürel, A., Armutçu, F., Kamisli, S., Iraz, M., Akyol, O. and Özen, S., "Gingko biloba prevents mobile phone-induced oxidative stress in rat brain", *Clinica Chemica Acta*, pp.153-162, No.340, 2004.

11. Özguner, F., Öktem, F., Ayata, A., Koyu, A. and Yilmaz, H.R., "A novel antioxidant agent caffeic acid phenetyl ester prevents long-term mobile phone exposure-induced renal impairment in rat", *Molecular and Cellular Biochemistry*, pp.73-80. No.277, 2005.

12. Anderson, D., "Antioxidant defences against reactive oxygen species causing genetic and other damage", *Mutation Research*, pp.103-108, No.350, 1995.

13. Simonian, N.A. and Coyle J.T., "Oxidative Stress in Neurodegenerative Diseases", *Annu Rev Pharmacol Toxicol*, pp.83-106, Vol.36, 1996.

14. Turner, R.N., "Free radicals and disease: the toxaemia hypothesis", *Complementary Therapies in Medicine*, pp.43-47, Vol.4, 1996.

15. Mahboob, M., Shireen, K.F., Atkinson, A., "Lipid peroxidation and antioxidant enzyme activity in different organs of mice exposed to low level of mercury", *J Environ Sci Health B.*, pp.687-697, Vol.36, 2001.

16. Maritim, A.C., Sanders, R.A., Watkins, J.B. 3rd., "Diabetes, oxidative stress, and antioxidants: A review", *J Biochem Mol Toxicol*, pp.24-38, Vol.17, 2003.

17. Stadtman, E.R., "The Role of Free Radical Mediation of Protein Oxidation in Aging and Disease". In Özben T (eds.): *Free Radicals, Oxidative Stress, and Antioxidants*, pp.131-143, Plenum Press, New York, 1998.

18. Coyle, J.T. and Puttfarcken, P., "Oxidative Stress, Glutamate and Neurodegenerative Disorders", *Science*, pp.689-694, No.262, 1993.

19. GSM Association website. (http://www.gsmworld.com)

20. ETSI/TC SMG, Recommendation GSM 05.05 Radio Transmission and Reception**,** October 1993, version 3.16.0.

21. Harte, L., Levine, R. and Livingston, G., *GSM Superphones*, McGraw-Hill, New York, 1999.

22. Hanzo, L., "The Pan-European Cellular System", in *Telecommunications Handbook*, Terplan, K and Morreale P. (eds.), pp.1226-1245, CRC Press, 2000.

23. Health Council of the Netherlands: GSM Base Stations. The Hague: Health Council of the Netherlands, pub.no.2000/16E, 2000

24. COMAR Reports, "Safety Issues associated with Base Stations Used for Personal Wireless Communications – A COMAR Technical Information Statement", *IEEE Engineering in Medicine and Biology Magazine*, Vol.20, No.2, pp.110-114, 2001

25. UK Mobile Operators Association website. (http://www.mobilemastinfo.com).

26. Cooper, T.G., Mann, S.M., Khalid, M. and Blackwell, R.P., "NRPB W62 - Exposure of the General Public to Radio Waves near Microcell and Picocell Base Stations for Mobile Telecommunications", National Radiological Protection Board, September 2004.

27. Habash, R.W.Y., *Electromagnetic Fields and Radiation – Human Bioeffects and Safety*, Marcel Dekker Inc., New York, 2002.

28. Kathrein Werke KG, Eurocell Panel Type 732448 Product Sheet.

29. Neubauer, G., Röösli, M., Feychting, M., Hamnerius, Y., Kheifets, L., Kuster, N., Ruiz, I., Schüz, J., Überbacher, R., Wiart, J., "Study on the Feasibility of Epidemiological Studies on Health Effects of Mobile Telephone Base Stations – Final Report", FSM – Project No. A2003-9, ARC-IT-0124, March 2005.

30. Verum Foundation, "REFLEX Project Final Report - Risk Evaluation of Potential Environmental Hazards From Low Frequency Electromagnetic Field Exposure Using Sensitive in vitro Methods", 31 May 2004.

31. Health Council of the Netherlands: Mobile telephones. An evaluation of health effects. Publication Number 2002/01E, 2002.

32. Uysal, M., "Serbest Radikaller, Lipit Peroksitleri ve Organizmada Prooksidan-Antioksidan Dengeyi Etkileyen Kosullar", *Klinik Gelisim*, pp.336-341, Vol.11, 1998.

33. Sözmen, E.Y., "Yaslanma Biyokimyasi", in *Insan Biyokimyasi*, Sözmen E.Y., Emerk K., Onat T. (Eds)., pp.665-674, Palme Yayincilik, Ankara, 2002.

34. Fang, Y., Yang, S. and Wu, G., "Free radicals, Antioxidants and Nutrition", *Nutrition*, pp.872-879, Vol.18, 2002.

35. Fridovich, I., "Superoxide radical and superoxide dismutases", *Annu Rev Biochem*, Vol. 64, pp.97-112, 1995.

36. Baboir B.M., "The respiratory burst of phagocytes", *J Clin Invest*, No.73, pp.599, 1984.

37. Asada, K. and Kiso, K., "Initiation of aerobic oxidation of sulfite by illuminated spinach chloroplasts", *Eur J Biochem*, Vol.33, No.2, pp.253–257, 1973.

38. Halliwell, B., "Antioxidants Characterization - Methodology and Mechanisms", *Biochemical Pharmacology*, Vol.49, No.10, pp.1341-1348, 1995.

39. Yalçin, S., "Antioksidanlar", *Klinik Gelisim*, Vol.11, pp.342-346, 1998.

40. Halliwell, B., Aeschbach R., Löliger J. and Aruoma O.I., "The Characterization of Antioxidants", *Fd Chem Toxic*, Vol.33, No.7, pp.601-607, 1995.

41. Fridovich, I., "Biological effects of the superoxide radical", Arch Biochem Biophys, Vol 247, No.1., pp.1-13, 1986.

42. Singh, R.J., "Editorial - Glutathione: A marker and antioxidant for aging", *J Lab Clin Med*, pp. 380-381, Vol.140, No.6, 2002.

43. Lang, C.A., Mills, B.J., Mastropaolo, W. and Liu, M.C., "Blood glutathione decreases in chronic diseases**",** *J Lab Clin Med*, Volume 135, Number 5, 2000.

44. Yürekli, A.I., Özkan, M., Kalkan T., Yazici, M., Seker, S. and Saybasili, H., "Dosimetry Measurement and Computation of an Experiment Setup Developed for Base Transceiver Station Exposure", *Proceedings of the 2nd International Workshop on Biological Effects of Electromagnetic Fields*, Rhodes, 2002.

45. National Research Council, "Guide for the Care and Use of Laboratory Animals", National Academy Press, Washington, D.C., 1996.

46. Yi, Sun, Oberley, L.W., Ying, Li,. "A simple method for clinical assay of superoxide dismutase", *Clinical Chemistry*, pp.497-500, Vol.34, 1988.

47. Burtis, C.A., Ashwood, E.R., Tietz, N.W., "Tietz Textbook of Clinical Chemistry", W.B. Saunders Company, 3rd Ed., 1999.

48. Satyanarayana, S., Srinivas, N., Rajabhanu, K., Sushruta K. and Krishna M.B., "Adaptogenic and nootropic activities of aqueous extract of Vitis vinifera (grape seed): an experimental study in rat model", *BMC Complement Altern Med*, Vol.5, No.1, 2005.

49. Yürekli, A.I., Özkan, M., Kalkan T., Saybasili, H., Tuncel, H., Atukeren, P., Gümüstas, K. and Seker, S., "GSM Base Station Electromagnetic Radiation and Oxidative Stress in Rats", *Electromagnetic Biology and Medicine*, Vol.25, pp.177-188, 2006.

50. Yürekli, A.I., Özkan, M., Kalkan T., Saybasili, H., Tuncel, H., Atukeren, P., Gümüstas, K. and Seker, S., "Effects Of GSM Base Station Electromagnetic Radiation On Oxidative Stress In Rats", *Proceedings of the 4th International Workshop on Biological Effects of Electromagnetic Fields*, Crete, 2006.

51. Dominguez-Gerpe, L. and Rey-Mendez, M., "Alterations induced by chronic stress in lymphocyte subsets of blood and primary and secondary immune organs of mice", *BMC Immunol.*, Vol.2, No.7, 2001.

52. Dhabhar, F. S., Miller, A. H., Stein, M., Mcewen, B. S. and Spencer R. L., "Diurnal and Acute Stress-Induced Changes in Distribution of Peripheral Blood Leukocyte Subpopulations", *Brain, Behavior, and Immunity*, Vol. 8, No.1, pp.66-79 , 1994.

53. Shi, Y., Devadas, S., Greeneltch, K. M., Yin, D., Allan Mufson, R., Zhou, J., "Stressed to death: Implication of lymphocyte apoptosis for psychoneuroimmunology", *Brain, Behavior, and Immunity*, Vol.17, No.1 supplement, pp.18-26, 2003.

54. Medical Encyclopedia, "VMA: What abnormal results mean", US National Library of Medicine & National Institute of Health, Bethesda, MD, A.D.A.M. Inc. Available at: http://www.nlm.nih.gov/medlineplus/ency/article/003613.htm#Normal%20Values

55. Moustapha, Y.M., Moustapha, R.M., Belacy, A., Abou-El-Ela, S.H., Ali, F.M., "Effects of acute exposure to radiofrequency fields of cellular phoneson plasma lipid peroxide and antioxidase activities in human erythrocytes", *Journal of Pharmaceutical and Biomedical Analysis*, pp. 605-608, Vol. 26, 2001.

56. Irmak, K., Fadillioglu, E., Güleç, M., Erdogan, H., Yagmurca, M., Akyol, O., "Effects of electromagnetic radiation from a cellular telephone on the oxidant and antioxidant levels in rabbits", *Cell Biochemistry and Function*, pp.279-283, Vol.20, 2002.

57. Cassarino, D.S., Fall, C.P., Swerdlow, R.H., Smith, T.S., Halvorsen, E.M., Miller, S.W., Parks, J.P., Parker, W.D., Bennett, J.P., "Elevated Reactive Oxygen Species and Antioxidant Enzyme Activities in Animal and Cellular Models of Parkinson's Disease", *Biochimica et Biophysica Acta*, pp.77-86, No.1362, 1997.

58. Thiffault, C., Aumont N., Quirion R., Poirier J., "Effect of MPTP and L-Deprenyl on Antioxidant Enzymes and Lipid Peroxidation Levels in Mouse Brain", *Journal of Neurochemistry*, pp.2725-2733, Vol.65, 1995.

59. Aoyama, K., Suh, S.W., Hamby, A.M., Liu, J., Chan, W.Y., Chen, Y., Swanson, R..A., "Neuronal glutahione deficiency and age dependent neurodegeneration in the EAAC1 deficient mice", *Nature Neuroscienc*e, pp.110-126, Vol. 9, 2005.

60. Amstad, P., Moret, R., Cerutti, P., "Glutathione Peroxidase Compensates for the Hypersensitivity of Cu, Zn-Superoxide Dismutase Overproducers to Oxidant Stress", *J Biol Chem*, pp.1606-1609, No. 269, 1994.

61. Yürekli, A.I. and Türetken, B., "RF field measurement and theoretical calculation for cellular base station antennas", *Proceedings of IV International Symposium on Electromagnetic Compatibility and Electromagnetic Ecology*, pp. 320-323, June 19-22, 2001, Saint-Petersburg, Russia.

62. Kuster, N. and Balzano, Q., "Experimental and Numerical Dosimetry" in *Mobile Communications Safety*, Kuster, N., Balzano, Q. and Lin, J.C (eds), pp.13-58, Chapman&Hall, 1997.

63. CENELEC, "ES 59005 - Considerations for the Evaluation of Human Exposure to Electromagnetic Fields (EMFs) from Mobile Telecommunication Equipment (MTE) in the Frequency Range 30 MHz – 6 GHz", October 1998.